Swansea University
Prifysgol Abertawe

Cronfa
Setting Research Free

Cronfa - Swansea University Open Access Repository

_____

This is an author produced version of a paper published in :
Desalination

_____

Cronfa URL for this paper:
http://cronfa.swan.ac.uk/Record/cronfa29220

_____

Paper:

Wang, K., Abdalla, A., Khaleel, M., Khraisheh , M. & Hilal, N. (2016). Mechanical properties of water desalination and wastewater treatment membranes. *Desalination*

http://dx.doi.org/10.1016/j.desal.2016.06.032

_____

Mechanical properties of water desalination and wastewater treatment membranes

Kui Wang[1], Ahmed A. Abdala[1, 2], Mohammad A. Khaleel[3], Nidal Hilal[1,4], Marwan K. Khraisheh[1,*]

[1]*Qatar Environment and Energy Research Institute (QEERI), Hamad Bin Khalifa University (HBKU), Qatar Foundation, PO Box 5825, Doha, Qatar*

[2]*College of Science and Engineering, Hamad Bin Khalifa University (HBKU), Qatar Foundation, PO Box 5825, Doha, Qatar*

[3]*Oak Ridge National Laboratory, Oak Ridge, TN 37831-6163, USA*

[4]*Centre for Water Advanced Technologies and Environmental Research (CWATER), College of Engineering, Swansea University, Swansea SA2 8PP, United Kingdom*

Abstract

Applications of membrane technology in water desalination and wastewater treatment have increased significantly in the past few decades due to its many advantages over other water treatment technologies. Water treatment membranes provide high flux and contaminant rejection ability and require good mechanical strength and durability. Thus, assessing the mechanical properties of water treatment membranes is critical not only to their design, but also for studying their failure mechanisms, including the surface damage, mechanical and chemical ageing, delamination and loss of dimensional stability of the membranes. The various experimental techniques to assess the mechanical properties of wastewater treatment and desalination membranes are reviewed. Uniaxial tensile test, bending test, dynamic mechanical analysis, nanoindentation and bursting tests are the most widely used mechanical characterization methods for water treatment membranes. Mechanical degradations induced by fouling, chemical cleaning as well as membrane delamination are then discussed. Moreover, in order to study the membranes mechanical responses under similar loading conditions, the stress-state of the membranes are analyzed and advanced mechanical testing approaches are proposed. Some perspectives are highlighted to study the structure-properties relationship for wastewater treatment and water desalination membranes.

Key words: Membrane; Wastewater treatment; Desalination; Stress state; Mechanical characterization; Mechanical properties

* Corresponding author: E-mail address: mkhraisheh@qf.org.qa (M.K. Khraisheh).

1

HIGHLIGHTS

- Experimental techniques to assess the mechanical properties of water treatment membranes are reviewed.
- Mechanical degradation mechanisms of water treatment membranes are discussed.
- Stress-state of the water treatment membranes are analyzed at different scales.
- Advanced mechanical testing methods are proposed to study structure-properties relationship for water treatment membranes.

Table of Contents

Abbreviations

AFM	Atomic force microscopy	APDSPO	bis(4′-aminopropyldiethoxysilylphenyl) 1,3,4-oxadiazole
AQPz	Aquaporin Z	CA	Cellulose acetate
CFD	Computational fluid dynamics	CMS	Chloromethyl styrene
CNF	carbon nanofiber	CNT	Carbon nanotube
DG	Diethylene glycol	DIC	Digital image correlation
DMPC	1,2-dimyristoyl-sn-glycero-3-phosphocholine	DMA	Dynamic mechanical analysis
DVB	Divinylbenzene	FEP	poly(tetrafluoroethylene-co-hexafluoropropylene)
GO	graphene oxide	hPI	hydrogenated polyisoprene
MBF	multibore hollow fiber	MBR	Membrane bioreactor
MD	Membrane distillation	MF	microfiltration
NF	Nanofiltration	NMP	N-methyl-2-pyrrolidone
PA	Polyamide	PAA	Polyacrylic acid
PAI	poly(amide–imide)	PAN	polyacrylonitrile
PEG	polyethylene glycol	PEI	Poly(ethyleneimine)
PES	polyethersulfone	PET	Polyethylene terephthalate
PLA	Poly (lactic acid)	PP	polypropylene
PRO	Pressure retarded osmosis	PS	polystyrene
PSF	polysulfone	PVA	poly(vinyl alcohol)
PVDF	polyvinylidenefluoride	PVDF-HFP	polyvinylidenefluoride-co-hexafluoropropylene
RO	Reverse osmosis	SAXS	Small-angle X-ray scattering
SBF	single-bore hollow fiber membrane	SEM	Scanning electron microscope
TFC	Thin film composite	UF	Ultrafiltration
VMD	vacuum membrane distillation	WAXS	Wide-angle X-ray scattering
ZrDETPMP	Zirconium diethylene triamine pentamethylene phosphonic acid		

1. Introduction

Although 72% of the earth is covered with water, 97% of that is salty seawater, which is not suitable for domestic and industrial applications. Moreover, 70% of the rest 3% fresh water is locked in ice and not accessible. Nowadays, the growing population results in an increasing demand on the quantity and quality of drinking water, especially in water-stressed countries. In the meantime, some existing groundwater and rivers are gradually polluted and unavailable due to industrialization and urbanization [1]. Therefore, global fresh water shortage is becoming the most serious problem affecting the economic and social development [2]. Attention is focused on the development of more sustainable technological solutions that are able to meet the increasing water consumption of future generations. Seawater desalination and wastewater treatment are the main technologies for producing clean water. Conventional desalination processes are generally based on thermal processes consuming substantial amount of energy with large greenhouse gases emission [3]. An environmental-friendly method for water purifying at low cost, with less energy and with less chemicals is therefore more attractive and desirable.

Membrane technology is favored over other approaches for desalination and wastewater purification due to its promising high efficiency, ease of operation, energy and space saving, and the no use of chemicals. Membrane filtration for water treatment has increased significantly in the past few decades with the enhanced membrane quality and decreased membrane costs. This method is a separation process that uses a semipermeable membrane to divide the feed stream into a desirable permeate stream that passes through the membrane walls and a retentate stream containing high concentration of rejected species [4], [5], [6] and [7].

Most of the reported research that deals with seawater desalination or wastewater treatment membranes focuses on membrane processing [8] and [9], surface modification[10] and [11], and antifouling properties [12] and [13]. More recently, molecular dynamics simulations of the physical and mechanical properties for nanoporous graphene membrane were conducted [14], [15], [16], [17] and [18]. However, experimental investigations of the mechanical behaviors under complex loading modes with temperature and pressure effects for porous membranes are rarely reported. According to Scopus database, the annual publications on desalination and water treatment membranes has grown from 1050 publications in 2004 to nearly 2500 publications in 2014. On the other hand, the number of annual publications that investigate the mechanical properties of desalination and water treatment membranes, regardless of being increased from 20 publications in 2004 to about 100 publications in 2014, is still represents less than 5% of the annual desalination and water treatment membranes publications.

In addition to high permeate flux, high contaminant rejection, good chemical and fouling resistances, water treatment membranes require good mechanical stability and durability. Membrane processes end users require a suite of techniques to independently assess the properties of the membranes received from the manufacturer before commissioning the process and at different stages during the membrane life (for diagnosing performance). Thus, analysis of the membrane real loading conditions and examining their mechanical properties under similar conditions are very important. Furthermore, understanding the mechanical behaviors of water treatment membranes with underlying deformation mechanisms is critical not only for designing membrane structure, but also for predicting membrane failures including: 1. Complete breakage (which is very rare); 2. Surface damage (impingement by sharp particles); 3. Cracking (due to insufficient flexibility of the membrane, this particularly affects outside feed formats that use air scour in backwash and for inside feed formats, a lack of compression strength will cause the fiber to crack since it cannot withstand the high flow and pressure in backwash); 4. Dimensional stability (can create disengagement in hollow fiber formats of the membrane from the potting tube-sheet if the membrane shrinks, and can create delamination in composite membranes); 5. Aging (mechanical fatigue and chemical attack due to hydrolysis which can be accelerated by high or low pH. Note that both mechanical fatigue and chemical attack can result in mechanical degradation of polymeric membrane by chain scission mechanism. However, cracks induced by mechanical ageing may initiate at the surface or inside the membranes, while cracks induced by chemical attack can only initiate at the membrane surface [19].)

This article reviews the most widely used experimental techniques for characterizing the mechanical behaviors of desalination and wastewater treatment membranes. Moreover, the mechanisms responsible for the mechanical degradations of these membranes are also discussed. In order to study the mechanical responses of membranes under real operating conditions, the stress-state at both lab and commercial scales is discussed. Finally, some advanced mechanical testing methods are proposed with potential real-time monitoring techniques.

Desalination and wastewater treatment membranes can be classified according to their pore size, mechanisms of rejection, driving forces, composition of membranes, geometry and configuration [20]. According to pore size, wastewater treatment and desalination membranes are classified as microfiltration (MF), ultrafiltration (UF), nanofiltration (NF) and reverse osmosis (RO) membranes. Among these membranes, RO membranes has much tighter pore structure that can effectively remove a wide range of ions from water, but requires the highest differential pressure (30–60 bar). Because of its very small pore size, RO has low permeate flux and is usually used for seawater desalination [20]. RO is considered the most energy-efficient water treatment technology in chemical and environmental applications and RO desalination is

the primary choice for seawater desalination, dominating about 45% of the total global desalination technology[3] and [21].

According to their material of construction, wastewater treatment and water desalination membranes are classified as inorganic, organic (polymeric), and hybrid membranes. Inorganic membranes are based on either metallic or ceramic materials and they are used for MF and UF membranes. Their high chemical and thermal stability make them suitable for use in corrosive and high temperature environments. However, ceramic membranes have few commercial applications due to their mechanical fragility and relatively high cost and metallic membranes usage is limited to gas separation. Polymers remain the most widely used material for commercial water treatment membranes due to their good separation performance. Polymeric membranes such as polyvinylidene fluoride (PVDF), polyacrylonitrile (PAN), polyethersulfone (PES) and polyamide (PA) are the most used membranes. However, polymeric materials are very susceptible to thermal, chemical and biological degradation [22]. Blending polymers or composite of polymers with inorganic fillers are effective method to provide new and better polymer based membranes to meet the requirements of many practical applications. The blended membranes can posses a range of chemical, physical and mechanical properties, making blending a favorable approach due to its versatility and simplicity. Recently, the use of nanoparticles to enhance the performance of membranes has been successful attempted by incorporating nanofillers into ceramic or polymeric membranes, leading to breakthrough performance related to fouling mitigation, improvement of permeate quality and flux enhancement [23], [24], [25] and [26].

For membrane configurations, the spiral wound module is the dominant product type for RO application. In spiral wound configuration, flat sheet membranes are usually wrapped around a central collection permeate tube with a sandwich structure. This configuration can reduce concentration polarization, fouling, and particle cake deposition. However, spiral wound configuration is defenseless to biofouling occurrence [27] and [28]. Moreover, the seals and glue lines are weak points which may result in the loss of module integrity. Hollow fiber membranes are mostly based on PVDF and PES and are usually submerged in a basin or pressurized in housing for UF and RO applications. Hollow fiber membranes for UF applications are arranged in rectangular modules which form a cassette and directly immersed into an aeration basin for membrane bioreactor (MBR). If RO is used in the hollow fiber configuration, numbers of hollow fibers are tightly bundled and bonded at the end housed in a tube. Table 1 summarizes the applications, the materials and the configurations for water treatment membranes. In this table, we also resumed the most used mechanical approaches for investigating the mechanical behavior of the membranes and how these results can be used in the application.

7

2. Membranes and membrane materials

The essential requirements for a common mechanical testing are controllable change in the specimen displacement and displacement speed and a mean to accurately measure the corresponding change in required load. The material stress–strain behavior can be obtained from the measured forces and displacements based on the sample cross section area and loading mode [29].

Conventional tests are difficult to directly apply for studying the mechanical properties of membranes because of their small thickness. For bulk materials, mechanical testing provides average properties over a large specimen cross-section and the specimen dimensions usually do not interfere with fundamental length scale [30]. Whereas the membrane sample size is usually quite small, it is therefore expected that the mechanical responses of the membranes exhibit a sample size dependence [31]. The strain-induced microstructural changes for membranes are often significant, invalidating many assumptions, such as in-plane elastic isotropy made about plastic deformation of bulk materials. Therefore, the mechanical properties of membranes need to be accurately evaluated with the underlying mechanisms, in order to optimize the membrane design and processing, to be used with long service time. Current methods to study the mechanical behaviors of wastewater treatment and seawater desalination membranes include uniaxial tensile testing, bending test, dynamic mechanical analysis, depth-sensing nanoindentation and bursting tests. Table 2 summarizes the most used approaches to study the mechanical properties of the water treatment membranes and the reported mechanical behaviors by using these methods. By using these methods, elastic, plastic, viscoelastic, hardness, as well as fracture and toughness properties can be determined. In the following sections, the major aspects of each technique are highlighted.

2.1. Uniaxial tensile test

Uniaxial tensile testing is one of the fundamental and the most used testing methods to investigate the mechanical behaviors of materials. In uniaxial tensile test, the specimen is stretched at a controlled constant tensile speed until a given strain or failure occurs. From the

8

measured load (F), displacement (Δl), the original specimen cross-sectional area (S_0) and initial length (l_0), the engineering/nominal stress ($\sigma eng = F/S_0$) and strain ($\varepsilon eng = \Delta l/l_0$) are determined. The true stress is the applied load acting on the instantaneous cross-sectional area. Assuming the material volume remains constant, then the engineering stress and strain can be used to derive the true stress–true strain curve, up to the strain at which necking begins, as follows [102] and [103]:

$$\varepsilon true = \ln(1 + \varepsilon eng) \qquad\qquad \text{equation(1)}$$

$$\sigma true = \sigma eng(1 + \varepsilon eng). \qquad\qquad \text{equation(2)}$$

Other important mechanical parameters such as Young's modulus, yield stress, strain-softening and strain-hardening characteristics, and ultimate stress and strain of materials can be obtained directly from the stress–strain curves. In addition, the area under the stress–strain curve determines the material toughness which relates to the material energy absorption capacity [104]:

Uniaxial tensile test is the most widely used mechanical testing method for wastewater treatment and seawater desalination membranes. For flat sheet membranes, the nominal/engineering stress can be determined as using the original cross sectional area, but for hollow fiber membranes, $\sigma eng_{(hollow\ fiber)}$ should be calculated according to their sectional surface area [96]:

$$\sigma_{eng\ (hollowfiber)} = \frac{F}{\dfrac{\pi\left(d_o^2 - d_i^2\right)}{4}} \qquad\qquad \text{equation(3)}$$

where do and di are the outer and inner diameter of the hollow fiber, respectively.

It is worth mentioning that there is currently no specific test standard for studying the mechanical properties of water treatment membranes. This is because that on the one hand, RO, NF, UF and MF are all used in different configurations that experience different mechanical loads. On the other hand, in some cases these testing methods for measuring intrinsic properties are derived from features of the membrane materials. For example, ASTM D6908 describes different techniques to test the integrity of membranes which is a function of mechanical properties. Nevertheless, ASTM D882-12 and ISO 527-3 for testing the tensile properties of thin plastic sheets (thickness less than 1 mm)[105] and [106] are the closest possible standards. Few studies have followed standard tensile test methods designed for thicker polymer specimens (ISO 6239 and ASTM D638) [107] and [108] or metallic materials (GB/T228-2002) [109].

9

Ahmed et al. [110] studied the mechanical strength of cellulose/electrospum polyvinylidenefluoride-*co*-hexafluoropropylene (PVDF-HFP) composite flat sheet membranes for efficient oil–water separation using uniaxial tensile test with dog-bone specimens (Fig. 1(a)). The tensile tests were conducted at a speed of 1 mm/min. The results showed that the addition of up to 15 wt.% cellulose led to increase in the elastic modulus and tensile strength of the electrospun PVDF-HFP membranes (Fig. 1(b)). However, the elongation at break decreased with increasing the cellulose content (Fig. 1(c)). The change in the mechanical properties was due to the entrapment of the PVDF-HFP fibers in the cellulose matrix and their inability of their chains to easily reorient. Therefore, the elastic modulus and tensile strength increased. At cellulose content above 15 wt.%, the membranes suffered process-induced defects such as cracks during the drying step, which led to a decreased membrane stiffness.

Wang et al. [111] investigated the mechanical properties of novel graphene oxide (GO)-blended PVDF UF membrane at room temperature using uniaxial tensile testing at a speed of 2 mm/min. The tensile strength of PVDF/GO membrane increased with increasing the contents of GO up to 0.2 wt.%, and then it gradually decreased. The increase in tensile strength was attributed to the excellent mechanical properties of GO and the very high surface area and aspect ratio. Below GO content of 0.2 wt.%, GO was dispersed very well in PVDF matrix, improving the mechanical properties of the membrane. With further increase in GO content, GO aggregation and possibly weak interface led to a decrease in the tensile strength.

Han et al. [112] studied the mechanical behavior of a PA thin film composite (TFC) pressure retarded osmosis (PRO) membrane for renewable salinity-gradient energy generation using uniaxial tension experimental technique. The flat sheet of PA TFC membranes with 5 mm width and with 30 mm initial gauge length were tested under a tensile rate of 10 mm/min. Test temperature was not mentioned. The developed membranes exhibited very high toughness which was an important factor for the membranes outstanding compressive resistance properties.

A slightly higher tensile crosshead speed, 20 mm/min, was used to test the room temperature mechanical properties of polysulfone (PSF) UF membranes with polyethylene glycol (PEG) additive [113]. Increasing the dosage of PEG-400 (average molecular weight 400 Da) led to increased membrane porosity consequently decreasing the tensile stress at break. On the other hand, the elongation at break initially increased then decreased with increasing PEG-400 content. Increasing the PEG molecular weight, increased the elongation at break, while the tensile strength increased till to the PEG molecular weight of 1500 Da and then decreased. This was due to that appropriate increase in molecular weight of PEG could suppress the formation of macrovoids and enhance the mechanical strength. However, when the molecular weight of PEG

10

was high, the rapid increase of porosity arising from the increase in molecular weight of PEG addition might decrease the mechanical strength.

Universal testing machine with a crosshead speed of 50 mm/min was used to evaluate the mechanical strength of a self-supporting electrospun PAN nanofibrous membrane for water purification [114]. The obtained stress–strain curve exhibited a nonlinear relationship between the applied stress and deformation. The measured mechanical properties indicated that this membrane could serve as a self-supporting membrane for fluid streams.

Uniaxial tensile testing is also widely used to identify mechanical behaviors of ductile polymer membranes and polymer matrix membranes [32], [34], [35], [36], [40], [44], [46],[47], [48], [53], [58], [61], [94] and [115]. However, the focus of most of the studies was to correlate the mechanical properties with the processing conditions or the composite composition or loading. No significant attempts were made to correlate the mechanical properties of the membrane to its operational performance, reliability, and lifetime. Moreover, the majority of the studies did not follow any standards with regard to the test specimen and the crosshead speed. For example, the grip distance was varied between 20 mm [35] to 100 mm [36] and [115] and the crosshead speed was varied between 2 mm/min [44] to 500 mm/min [115] depending on the initial gauge length and initial sample length. In addition, most of the uniaxial tensile tests were carried at room temperature and not the temperature at which the membrane will operate.

Although uniaxial tensile is the most used mechanical testing method for thin films [97],[116], [117], [118], [119] and [120], due to the delicacy and very thin thickness of the membrane materials, the following must be considered while using uniaxial tensile test for membrane testing: (1) dog-bone/dumbbell specimen is recommended to avoid specimen rupture around the gripped sections due to stress concentration induced by clamping (Fig. 1(a)), (2) suitable grip and grip serrated surface should be used to avoid tearing/fracture the specimen around the gripped area rather than at the middle of the specimen, (3) The vertical alignment of the membrane samples and the grips should be adjusted to avoid side loading or bending, and (4) clamping force should be adaptable to avoid slippage or damage of the gripped membrane during operations.

2.2. Bending test

Bending or flexure testing is an important mechanical testing method to define the ability of relatively brittle materials to resist deformation when subjected to simple beam loading and the

11

results are presented in a stress - strain curve. The flexural strength represents the highest stress before the material ruptures. According to the loading point, bending test can be divided into 3 - point and 4 - point flexure tests as shown in Fig. 2.

In a 3-point bending test, the specimen is placed on two parallel supporting pins and a third loading pin is lowered at the specimen mid-point at a constant speed. For a rectangular cross-section specimen, the bending strength ($\sigma_{f3}r$) is calculated from Eq.(4).

$$\sigma_{f3r} = \frac{3FL}{2bd^2}$$

equation(4)

For a hollow fiber, the 3-point bending strength ($\sigma_{f3}h$) is given by Eq. (5)[121]:

$$\sigma_{f3h} = \frac{8FLd_o}{\pi\left(d_0^4 - d_i^4\right)}$$

equation(5)

where F is the measured force at a given point on the deflection curve, L is the support span. b and d are the rectangular beam width and depth, respectively. *do* and *di* are the outside and inside diameters of hollow fiber, respectively.

In contrast to 3-point bending test, 4-point bending test requires the sample to be placed on two supporting pins. Two loading pins are placed at an equal distance around the center. For a rectangular cross-sectional specimen, the flexure strength is calculated by:

$$\sigma_{f4r} = \frac{3Fa}{2bd^2} \cdot$$

equation(6)

Here, a is the distance between the supporting and loading pins. For a hollow fiber, the 4-point bending strength can be described by Eq. (7)[122]:

$$\sigma_{f4h} = \frac{16FKD}{\pi\left(d_0^4 - d_i^4\right)}$$

equation(7)

Here, K indicates a half of the difference between the outer and inner span. Furthermore, bending test can be used to determine the facture toughness of materials, details about the theoretical background are reported elsewhere [123]. 3-Point and 4-point bending tests are usually used for rigid porous ceramic and metallic wastewater treatment and seawater desalination membranes. It is worth noting that the thickness of some inorganic materials is not as thin as polymeric membranes. In addition, bending test can provide the flexibility and the suitability of using a particular product in a configuration that requires air scour for backwash/cleaning.

12

Sarkar et al. [69] investigated the impacts of clay content and sintering temperature on the bending strength of a clay-alumina porous capillary support for filtration application. The 3-point bending test was performed using a span of 30 mm and a loading speed of 10 mm/min. The flexural strength of the clay-alumina porous composite membranes increased with increasing sintering temperature and with increasing clay content. The increased clay content favored the mullite formation which had a significant consolidation effect on the material at high temperature.

Kritikaki and Tsetsekou [66] studied the effect of adding small amounts of fine sol–gel derived nanoalumina on the bending strength of a micron-sized alumina powder for the production of highly porous ceramic. The bending test was carried out with 30 mm span and with 0.5 mm/min crosshead speed. The results showed that the membrane bending strength depended on γ-alumina nanopowder content, materials mixing methods and the sintering temperature (Fig. 3). More specifically, the bending strength of the membrane increased for low nanopowder content (4–6 wt.%) then decreased for median nanopowder content and finally increased at high nanopowder content (20 wt.%), whatever materials mixing method and sintering temperature. The evolution of the membrane bending strength as a function of the nanopowder content is related to the materials' interface, homogeneity as well as to the membrane porosity.

The mechanical behaviors of porous Al_2O_3 ceramics prepared from pure Al_2O_3 powder and mixtures with $Al(OH)_3$ particles were studied using three-point bending test by Deng et al. [68] using 3 mm × 4 mm × 40 mm specimens, with a span of 30 mm and crosshead speed of 0.5 mm/min. The fracture toughness was measured using the single-edge notched-beam test, with a notch depth of 2.0 mm, a notch width of 0.1 mm and with a span of 16 mm. Due to the strong grain bonding, the bending strength of the ceramics increased with the addition of $Al(OH)_3$. For highly porous Al_2O_3, the fracture toughness increased with the addition of $Al(OH)_3$. However, the addition of $Al(OH)_3$ did not improve the fracture toughness of low porosity ceramics. This is attributed to the fracture-mode transition from the intergranular, at high porosity, to transgranular, at low porosity.

Lee et al. [76] prepared a nickel hollow fiber membrane and used three-point bending test to study the effect of the sintering temperature on the bending strength of the membrane. Higher sintering temperature in the investigated temperature range from 1100 °C to 1300 °C significantly improved the bending strength of the hollow fiber membrane. Similar finding was reported by Nandi et al. [71] on flexural strength of low cost ceramic membranes based on kaolin for micro-filtration applications. The bending strength of the membrane increased from 3 MPa

for sintering at 850 °C to 8 MPa for sintering at 1000 °C. The mechanical strength improvement with sintering temperature was due to the densification of the materials at high sintering temperature [67], [72], [75] and [77].

2.3. Dynamic mechanical analysis

Dynamic mechanical analysis (DMA) is a very useful tool to investigate the viscoelastic behavior of viscoelastic materials including polymeric membranes. DMA generally involves applying a small dynamic deformation on a specimen of known geometry and measuring the corresponded stress, or alternatively applying a dynamic stress on the specimen and measuring the resulting strain. In most cases, deformation is the controlled input and stress is the measured output [124]. DMA measures the stiffness and damping of materials at various temperatures and frequencies. In addition, this approach can be also used to determine the transition temperatures corresponding to molecular motion or thermal transition. Moreover, DMA fatigue test can also be used to evaluate the degradation/ageing of membranes at various high cyclic load levels and under various specific conditions. Although DMA allows various loading moduli such as dynamic tension, compression, shearing, dual and single cantilever, dynamic tension is one of the most used modes to study the dynamic mechanical properties of wastewater treatment and seawater desalination membrane.

Chung et al. [78] studied the effect of the shear rate within the spinneret during hollow fiber spinning on the mechanical properties of UF PES based hollow fiber membranes using DMA. The hollow fiber samples were heated from room temperature to 250 °C at a heating rate of 3 °C/min and a frequency of 10 Hz. The storage and loss moduli of the obtained PES hollow fiber membrane increased with increasing shearing rate as shown in Fig. 4. This was attributed to the highly oriented polymer chains at higher processing shear rate, resulting in a higher potential energy and inherent stiffness.

To remove Pb^{2+} from industrial wastewater, poly(vinyl alcohol) (PVA) nanocomposite membranes were prepared with different loading of zirconium diethylene triamine pentamethylene phosphonate (ZrDETPMP). DMA was used to study the dynamic mechanical properties of this membrane between 30 °C and 300 °C with 10 °C/min heating rate. The membrane stiffness was found to increase with ZrDETPMP content. This increased membrane stiffness with ZrDETPMP content is due to the hydrogen bonding of the matrix –OH groups, the high degree of crosslinking, and attuned polymer network formation [81].

14

Zhang et al. [83] measured the storage modulus of a PVDF hollow fiber membrane with PVDF or PAN polymer coating layer using DMA operating at 1 Hz in the temperature range − 80 to 50 °C at a heating rate of 5 °C/min. The room temperature storage modulus of the reinforced membranes were lower than the untreated PVDF membrane probably due to the erosion effect of the polymer solution on the matrix surface during the coating processing.

Singh et al. [82] also used DMA to study the dynamic performance of NF membranes containing silica monomer precursor and PVA at temperature range from 30 to 320 °C with a heating rate of 10 °C/min under N_2 atmosphere. The stiffness of this membrane increased with silica content because the silica based filler reduced the porosity of the polymer matrix.

DMA can be used to obtain accurate dynamic mechanical responses of wastewater treatment and seawater desalination membranes as a function of time, temperature and frequency at a small dynamic strain or with a small dynamic force. However, the test should be carefully carried by selecting proper initial serrated force applied by DMA grips to avoid membrane slippage or damaging in the gripped section. Moreover, as polymer membranes stretches and becomes softer at high temperature, a proper strain rate should be selected for different temperature ranges.

2.4. Nanoindentation

Nanoindentation is a technique developed in the mid 70s of the last century to measure the elastic modulus, hardness, and fracture toughness of solid materials. Because of its high-resolution of the load–displacement data acquisition ability, it is now used for the mechanical characterization of small size materials [125] and [126]. For water treatment membranes, nanoindentation can be used to investigate surface mechanical properties, which are useful to investigate surface damage of the membranes induced by scaling. In a typical indentation test, a hard pyramidal or spherical indenter is pressed into a studied material where the applied force and the corresponded indenter displacement are recorded [29]. From the force–displacement curves obtained by instrumented indentation, the measured contact stiffness, S, is determined [126], [127],[128] and [129]:

$$S = \frac{dF}{dh} = \frac{2}{\sqrt{\pi}} E_r \sqrt{A_p(h_c)}$$

equation(8)

where F is the indentation load. h is the indentation depth and dF/dh is the slope of the tangent to the unloading curve at the maximum loading point (Fig. 5), and $Ap(hc)$ is the projected contact area of the hardness impression at the contact depth hc, which is calculated as follows:

15

$$A_p(h_c) = C_0 h_c^2 + C_1 h_c + C_2 h_c^{1/2} + C_3 h_c^{1/4} + C_4 h_c^{1/8} + C_5 h_c^{1/16} \qquad \text{equation(9)}$$

where the constants C_i ($i = 1, 2, 3, 4, 5$) can be determined by a series of indentations at different depths on a standard materials and employing curve-fitting procedure. The reduced modulus, E_r, which accounts for the elastic deformation occurs in both the specimen and the indenter, is given by:

$$\frac{1}{E_r} = \frac{(1-v_s^2)}{E_s} + \frac{(1-v_i^2)}{E_i} \qquad \text{equation(10)}$$

where E_s and v_s are the Young's modulus and Poisson's ratio for the sample, and E_i and v_i are the Young's modulus and Poisson's ratio for the indenter. The hardness, H, is defined as the maximum load, F_{max}, divided by the residual indentation area, A_r:

$$H = \frac{F_{max}}{A_r}. \qquad \text{equation(11)}$$

Yakub [87] studied the modulus and hardness of a porous ceramic membrane for removal of contaminants from water using nanoindentation. In this, loading and unloading rates of 5 μm/s were applied through a spherical indenter with a peak load of 1000 μN. Both the membrane modulus and hardness increased with decreasing the average pore size but did not have any clear relationship with the porosity. It revealed that the elastic modulus and hardness of the membrane were strongly influenced by the average membrane size rather than the porosity.

In order to evaluate the effect of the molecular structure on the mechanical properties of a cross-linked sulfonated block copolymer for water purification applications, nanoindentation testing was carried out by Yeo et al. [89]. The measurements were conducted under ambient atmosphere and the results indicated that the chemical cross-linking had a significant effect on the mechanical properties of the block copolymer due to the existence of chemical crosslinking in loop/bridge conformations. At a given stress, the chemical crosslinking made the materials more resistant.

The effect of GO on the strength of a nanohybrid NF membrane was analyzed by Wang et al. [90]. The results demonstrated that Young's modulus and hardness of the PAN substrate membrane have shown an insignificant change after hydrolysis (Fig. 6). However, a more pronounced change was observed with poly(ethyleneimine) (PEI)/polyacrylic acid (PAA) as Young's modulus and hardness significantly increased when PEI modified-GO/PAA was deposited on the membrane. These results also indicated that the mechanical behaviors of the composite membrane were improved by the addition of GO.

16

In recent years, atomic force microscopy (AFM) technique has shown a versatility in the characterization of surface properties of materials [130]. It allows high-resolution topography investigations as well as mapping of the elastic and viscoelastic behaviors of materials. In this technique, an AFM cantilever serves as a soft nanoindenter allowing local investigation of small and inhomogeneous specimen at the nanometric scale [131],[132] and [133]. Nevertheless, the use of this technique to study the mechanical properties of water treatment and desalination membranes is still limited.

Tai et al. [91] prepared a free-standing and flexible electrospun carbon-silica nanofibrous membrane for ultrafast gravity-driven oil–water separation. The Young's modulus of the single SiO_2–carbon composite nanofiber and the carbon nanofiber (CNF) was evaluated by contact mode AFM utilizing a silicon cantilever with a pyramidal tip. The force mapping of the fiber surface was conducted on a random area of $5 \times 5 \ \mu m^2$. The average Young's modulus for CNF was three times higher than that of SiO_2–carbon composite nanofiber suggesting that SiO_2–carbon composite nanofiber is more flexible than CNF.

Wang et al. [92] molecularly designed a pore-suspending biomimetic membrane embedded with Aquaporin Z (AQPz) based on different lipid protein ratios for water purification. The mechanical behavior of the membranes was studied by force indentation using AFM in the center of the unsupported membrane-covered pores with a constant piezo-electric velocity of 0.5 m/s at a temperature of $20 \pm 1 \ ^\circ C$ in water. It was reported that the mechanical properties of the membrane was improved by increasing the AQPz content, suggesting that AQPz increases the energy barrier required for a normal force to punch through the biomimetic membrane.

Nanoindentation is an effective technique to determine the mechanical properties of thin films and coatings. However, this method is usually used to study the local surface mechanical properties of the materials. Accuracy of determination of mechanical properties by nanoindentation can be effected by various factors, such as inadequate model for data processing or omission of some specific properties or factors, such as pileup, surface forces or temperature changes [134].

2.5. Bursting test

Bursting test can present a realistic reflection of the mechanical strength of flat sheet and hollow fiber wastewater treatment and seawater desalination membranes. It is a suitable mechanical testing method to determine the force required to rupture the membranes under a planar stress-state. In this test, the membrane is subjected to increased applied pressure till failure occurs. At

17

this point, the pressure is noted as the bursting pressure or bursting strength [97], [98], [135], [136] and [137].

To investigate the mechanical properties of a PVDF-HFP flat sheet membrane for direct contact membrane distillation, Lalia et al. [95] used a capillary flow porometer to perform the Mullen burst test with the setup as shown in Fig. 7(a). The membrane (50 mm × 50 mm) is clamped over a rubber diaphragm to keep the water from escaping the system or touching the membrane. With increasing the applied air pressure, the diaphragm is steadily pressurized with water. At the rupture of the membrane, the rubber diaphragm suddenly expand to the failure point of the membrane and the corresponding bursting strength is recorded by the software [99], [100] and [138]. The results obtained from the bursting test demonstrated that the burst pressure increased with increasing the concentration of PVDF-HFP used for electrospinning. This is attributed to the larger fiber diameter obtained at higher polymer solution concentration. The increase in fiber thickness ultimately increased the mechanical strength of the spun mats and hence of the membranes [95].

Bursting test can also be used to investigate the mechanical properties of hollow fiber membranes [93], [96] and [101]. Wang and Chung [93] carried out burst test using a laboratory fabricated setup to investigate the mechanical properties of PVDF multibore hollow fiber (MBF) membrane developed for vacuum membrane distillation (VMD). The laboratory setup for hollow fiber burst pressure measurement is shown in Fig. 7(b). A water reservoir with 3.5 wt.% NaCl solutions was used to provide the testing solution. Hydraulic pressure was provided by compressed N_2. The hollow fiber module was prepared by sealing one end of the fiber and leaving the other end open. The outlet of the tube was connected to the lumen side of the hollow fiber module. The whole module was put in a beaker of deionized water. During the test, hydraulic pressure was increased with a step of 0.1 bar. The conductivity of the water in the beaker was monitored by a conductivity meter in order to measure the liquid entry pressure. The burst pressure of the MBF membrane was much higher than that of the single-bore hollow fiber membrane (SBF), because of the larger overall cross-section area of the MBF membrane with its lotus-root-like structure which could maximize the mechanical stability at the radical direction. In addition, comparing the burst pressure of two MBF membranes with different spun conditions, they concluded that the burst pressure depends on the tightness of the inner-surface pore size. The tighter surface due to the smaller pore size exhibited higher burst pressure.

Zhang et al. [139] used a lab-scale RO setup to measure water permeability and burst strength of PES hollow fiber membrane. A deionized water was pumped into lumen side of the hollow fibers

at a flow rate of 0.15 ml/min and pressurized to 2 bar for 20 min before permeate was collected from the shell side. After measurement of the water permeability, the applied pressure was gradually increased at intervals of 3 bar below 14 bar and 1 bar above 14 bar. The water permeability was measured at each pressure. A decreased of water permeability versus pressure was observed due to the membrane densification until the membrane failed indicated by the sudden increase in the water permeability with the corresponding pressure noted as the burst pressure [139] and [140]. In addition, Zhang et al. related the burst pressure, P, to the tensile stress of hollow fiber membrane by using Barlow's formula for isotropic tubes [139]:

$$P = \frac{2t\sigma}{d_o \cdot S_f}$$
equation (12)

where t is the hollow fiber wall thickness, d_o is the outer diameter and S_f is the safety factor usually taking $S_f = 1$. σ refers to the membrane tensile stress. Thus, the burst strength of hollow fiber membrane strongly depends on the wall thickness, outer diameter and tensile stress of the membrane. By using this relationship between the burst pressure and tensile stress, Zhang et al. [139] estimated the burst pressure by using tensile stress comparing to the measured ones. It was found that the estimated burst pressure was slightly different from the measured burst pressure for a given PES hollow fiber membrane. The reason was attributed to the anisotropy of the hollow fiber membranes. Because of a hydraulic pressure was directly exerted upon the inner layer of the hollow fiber support during the burst pressure test, the porosity and thickness of the inner skin layer became especially important at high pressures. They therefore concluded that the mechanical strength of hollow fiber membranes were highly dependently not only on outer diameter and wall thickness (Eq. (10)), but also on porosity and the micro-structure of the membranes.

Liu et al. [96] studied the effect of reinforcing PVDF with PET threads on the mechanical strength of PVDF hollow fiber membrane using burst test. They reported that the addition of PET threads had little effect on the membrane burst pressure (Fig. 8). However, the burst pressure of the membrane increased significantly with increasing PVDF concentration in the dope solution for both the unreinforced and reinforced membranes due to the tighter stack of molecule chains in the membrane at a higher PVDF concentration. The addition of PET threads led to their distribution over the membrane along the axial direction. The diameter of PET threads was very small compared to the membrane girth and PET threads did not affect the microstructure of the membrane and consequently having a very small effect on the bursting pressure.

Bursting test is a useful mechanical testing approach to investigate the failure strength of wastewater treatment and seawater desalination membranes under planar stress-state. However, during the bursting test, only the failure pressure of the membranes is recorded. Therefore, the

19

relationship between the applied pressure and membrane deflection, which is important to analyze the microstructure evolution under an increasing applied pressure, cannot be established. In addition, the measured bursting pressure is highly dependent on the experimental protocol such as testing devices, data acquisition methods and step pressure. Similar to the effect of strain rate on the mechanical properties of polymer membranes using uniaxial tensile test, it is expected that a higher step pressure for the bursting test can yield a higher bursting strength of membranes[141].

3. Mechanical degradation of water treatment membranes

Mechanical strength plays an important role in reliability and durability of wastewater treatment and seawater desalination membranes. Mechanical degradation of membrane due to fouling, physical damage and chemical ageing induced by harsh source water, biological growth, physical pore blocking, backwashing, chemical cleaning could lead to a decrease of membranes' stiffness and strength [120], [142], [143], [144], [145],[146] and [147]. More specifically, mechanical degradation induced failure of membranes can cause a variation of applied pressure, flux, particle rejection and permeability, consequently, a loss of quality for permeate. Uniaxial tensile testing is the most used experimental technique to investigate the mechanical degradation of the membranes.

3.1. Fouling induced mechanical degradation

Membrane fouling is initiated by the accumulation of inorganic, organic, colloidal and biological species on the membrane surface and/or within its pores. It results in a reduced flux, a rapidly increased transmembrane pressure, and possibly deterioration of mechanical properties [1], [148], [149] and [150].

Nghiem and Schäfer [151] investigated the effect of fouling on the mechanical behaviors of hollow fiber MF membrane element taken from a water recycling plant by using uniaxial tensile test. A 200 mm long sample was characterized under a loading rate of 50 mm/min. Fig. 9 shows the elongation at break for five fouled samples in comparison with the virgin unfouled membranes. Fouled membranes are more brittle than the unfouled hollow fibers due to the normal wear and tear during the filtration process and backflush operations although the major foulant included colloidal particles and organic matters.

Zondervan et al. systematically analyzed the parameters that influenced membrane life-time by analysis of variance [144]. Mechanical investigation was performed using uniaxial tensile test

20

with a 10 N loading cell. They found that the elongation at break of fouled modules was nearly half of that of the clean modules indicating that fouling significantly influenced the membrane integrity.

3.2. Chemical cleaning induced mechanical degradation

To deal with membrane fouling, chemical cleaning has been proved as an effective method towards recovery of the original membrane permeability. Chemical cleaning has been accepted for foulant removal from membrane cell in large water treatment plants[148], [152], [153], [154], [155] and [156]. However, cleaning with chemical agents may not only remove foulants but also attack the membrane materials causing its mechanical degradation.

Arkhangelsky et al. studied the hypochlorite cleaning effect on the mechanical responses of a commercially available CA UF membrane using uniaxial tensile tests [157] and [158]. Wet membrane samples (76 mm × 5 mm × 0.2 mm) were clamped between two aluminum holders. A pre-stretching step (force 3 N for 5 s) was applied to stabilize the investigated samples. The CA membranes were then drawn at a constant crosshead speed of 0.001 m/s till break. The exposure of CA membranes to hypochlorite was found to decrease the ultimate tensile strength, ultimate elongation and elasticity modulus (Fig. 10). This mechanical degradation was more significant at higher hypochlorite dosage. The decreased mechanical properties were attributed to polymer chain breakage during the hypochlorite cleaning process.

Causserand et al. [159] and Rouaix et al. [160] simulated the chemical ageing of a PSF membranes by soaking them in chlorine solutions and then investigated their mechanical behaviors via uniaxial tensile test. Wet samples with a length of 200 mm were stretched at a speed of 200 mm/min and the results are shown in Fig. 11. The behavior of elongation at break for membranes immersed in hypochlorite is very sensitive to the solution temperature, to the solution pH value and the soaking time. More specifically, the elongation at break of these PSF membranes decreased with increasing temperature, and soaking time. The reduced mechanical

21

properties of PSF membranes were attributed to the polymer chain breakage during the expose to sodium hypochlorite.

3.3. Membranes delamination

Membrane delamination and formation of blisters between the layers are common problems in multi-layer membranes caused by the lack of proper adhesion between the active and supporting layers of flat sheet membranes [161]. For hollow fiber membranes, delamination possibly appears during membrane fabrication and it is caused by uneven shrinkages between inner and outer layers due to their different thermal properties, material incompatibility and different phase inversion rates [154] and [162]. Delamination during the membrane fabrication phase will result in macrovoids between different layers affecting the permeate quality. Under this condition, most studies have focused on improving the interface adhesion and preparing multi-layer membranes with initial delamination-free structures [163], [164] and [165]. In order to evaluate membrane resistance to failure, Hoover et al. [166] removed the spacer in their bench-scale laboratory equipment such that the failure points could be easily achieved with controlled pressure. With a water cross-flow velocities of 26 cm/s, they found that their wet-laid TFC membrane delaminated internally at the PET–PSF interface (Fig. 12). This interlayer delamination was attributed to the cross-flow induced shearing force applied on the membrane. The location of the delamination revealed that the membrane cell geometry affected the stress-state on the membranes [166].

4. Stress-state of polymeric membrane under actual condition

Inorganic membranes are typically designed as MF and UF to remove relatively large particles for water treatment purpose. Due to their inherent mechanical properties, inorganic membranes have good mechanical integrity during normal water treatment process. In contrast, polymer membranes with smaller pore size and higher efficiency for particle removal are widely used in seawater desalination with a high applied pressure. However, polymer membranes are mechanically weaker and have lower thermal and chemical stability compared to inorganic membranes. For next generation membranes, the materials should combine high permeability and high selectivity with sufficient mechanical stability [26]. Therefore, in the next sections, attention will be mainly focused on polymeric membranes operated under high pressure.

4.1. Flat sheet membranes

22

The mechanical performance of membranes depends not only on their material structure and fabrication method, but also on membrane module configuration. At laboratory-scale, cross-flow or tangential-flow filtration is commonly employed for flat sheet membranes. Within a single laboratory-scale cross-flow membrane cell, the solution to be filtered is pumped from the tank to the inlet of membrane cell with controlled pressure and flow rate. Flow then goes through the membrane cavity. During this process, the effect of shearing induced by the cross flow on the membrane can effectively remove the particles, reducing membrane fouling, and then maintaining a stable flux. The membrane sheet is generally positioned between a feed-side spacer and a permeate-side spacer. The central cavity between the cell bottom and cell top of the membrane depends on the thicknesses of the spacers. If the central cavity is too large, the membrane may wrinkle.

She et al. [167] studied the effect of spacer geometry on the performance of flat sheet membrane for PRO using a lab-scale cross-flow setup. They found that the spacer geometry had a significant effect on the membrane deformation. More specifically, the spacer with large mesh size could induce more severe membrane deformation at high pressure affecting the flow properties. Similar results were reported by Kim et al. [168]using a laboratory membrane cell to investigate the effect of feed channel spacer on the performance of PRO membranes. The results showed that the membrane was subjected to a tensile stress and with increasing tension induced by pressure, the active layer of the membrane would begin to crack and finally result in rupture of the membrane.

Cortés-Juan et al. [169] simulated the laminar fluid flow in a lab-scale flat circular filtration cell using computational fluid dynamics (CFD). The simulation results indicated that the flow direction, the velocity and the wall shear stress were strongly influenced by the membrane cell configuration. The addition of grooves on the top of the cell permitted to obtain intense velocity and wall shear stress fluctuations.

Flat sheet membranes for spiral wound configuration are sandwiched between feed channel spacers and permeate collection materials and rolled around a central collection permeate tube. The influence of spacer thickness on the permeate flux for seawater RO systems was experimentally investigated by Sablani et al. [170]. They found that the different geometry of the spacer might affect the turbulence at the membrane surface and a small thickness of spacer had less turbulence. The effect of spacer geometry on the flow properties for spiral-wound membrane

modules was also theoretically investigated by CFD simulations. The predictions revealed that the spacer filament configurations, mesh size, filament diameter and Reynolds number had complex effect on the flow direction, velocity and wall shear-stress [171] and [172]. The membranes are not only under simple shearing-stress condition induced by laminar flow but also under complex stress-state induced by turbulence flow [173] and [174]. The distribution of the shear-stress within spiral-wound membrane modules is fairly non-uniform because the spacer filaments create constrictions to the flow path [175]. For composite membrane used in a spiral wound configuration, high applied pressure can result in compaction of the polymer layer and membrane surface damage by the feed channel spacer, especially if the spacer moves relative to the membrane, which occurs each time when the system is pressurized and de-pressurized.

4.2. Hollow fiber membranes

Hollow fiber membrane configuration is mainly used for wastewater treatment applications and less commonly used in RO desalination processes, Nevertheless, when hollow fiber membranes are used for RO applications, they are usually housed into tubes and tightly bundled together with high packing density and therefore with less degree of freedom. Feed solution can be introduced in the center of fiber side or on the tube shell side. The permeate is withdrawn in a co-current or counter-current manner depending on the configuration of membrane module.

Kaya et al. [176] analyzed the wall shear-stress of an outside-in hollow fiber membrane modules by CFD simulation. The modeling results showed that the inlet and outlet of the membrane module could cause fluctuations in local velocity and on wall shear stress. The tangential inlet and outlet enabled rotational flow, providing slightly better wall shear stress on the fiber surfaces. The distribution of the shear-stress within hollow fiber membrane modules is inhomogeneous and the two ends have more complex stress-state induced by the multi-direction flow.

Therefore, flat sheet and hollow fiber membranes for wastewater treatment and seawater desalination operate under complex stress-state that depends not only on pressure and velocity distribution but also on the membrane cell configurations. The conventional methods to study the mechanical properties of the membranes do not represent the actual loading conditions. Therefore, advanced mechanical testing techniques should be developed to investigate the membranes under similar stress-state as that experienced in water treatment applications. A good start is to design and build a membrane mechanical testing cells that allow subjecting the

membrane to loading conditions similar to actual loading conditions at different scales and different cell configurations. The next challenge that requires to be overcome is to find an adaptable technique to continuously record the three-dimensional shape of the membranes under pressure and to correctly analyze the obtained load-deflection behaviors.

To fabricate spiral wound modules, multi-layer flat sheet membranes are rolled and the rolling radius could be small (the central permeate tubes may have a diameter of 2 cm). This small rolling radius may lead active polymer or functional coating layer to crack and bringing an earlier membrane failure. Bending test may be suitable to simulate the rolling process. Moreover, the study of the adhesion force between hollow fiber ends and resin by using pull out testing is also important to the mechanical integrity of hollow fiber membranes with tube configuration [120] and [156].

5. Advanced techniques for mechanical properties testing

5.1. Environmental effects on the mechanical properties of membranes

The mechanical behavior of polymers is very sensitive to temperature [104], [177], [178],[179] and [180]. More specifically, the yield stress and the Young's modulus decrease dramatically with increasing of temperature. Temperature effect on particle rejection[181] and [182], scaling [183], fouling [184], and permeate flux [185] of the water treatment membranes have been studied. However, investigation of the temperature effect on the mechanical properties of membranes is less reported. The middle-east, seawater temperature is higher than that of other countries [186]. Under these circumstances, the mechanical investigations of the membranes for seawater water RO application with temperature effects are especially important.

The pressure rate which depends on the duration required for the pressure to increase from zero to the maximum working pressure is also an important factor to study the mechanical responses of wastewater treatment and seawater desalination membranes. This effect is similar to the strain rate effect on the mechanical behavior of polymer where increased strain rate leads to material hardening to lower molecular chain mobility at large strain rates. More specifically, an increased pressure rate may influence the yield stress and the elastic modulus of the membranes resulting in an earlier material failure. Mechanical testing with high pressure rate can also use to simulate

the pressure shock on the mechanical responses of the membrane induced by operation or by system disturbances [187].

5.2. Membrane fatigue behavior

Membrane backwashing is an essential stage to remove foulants remaining membranes permeate and selectivity. During backwashing, the filtration process is reversed in which permeate is flushed through the membrane to the concentrate side. Backwashing can be done either by reducing the operation pressure below the osmotic pressure of the feed solution or by increasing the permeate pressure [188]. For the second case, the feed solution pressure should reduce to zero and then the permeate pressure is applied. Consequently, the water flux direction will be reversed, resulting in an opposite pressure loading and shearing applied to the membrane induced by tangential-flow. The frequency of backwashing, which could be high, depends on the type and rate of foulants build up on the membranes. In order to simulate the backwashing process, mechanical fatigue analyses should be conducted. To the best of our knowledge, no investigation about the fatigue behavior of wastewater treatment and desalination membranes under multi-axial loading conditions has been reported. Therefore, it is recommended to study the fatigue properties of the membranes under uniaxial loading state as well as bi-axial loading state with controlled environmental conditions and at various frequencies. Moreover, because some fouling particles need additional chemically enhanced backwash to remove, the fatigue tests can be conducted at different temperatures while the membrane sample is immersed in a cleaning solution medium. By using this approach, the mechanical fatigue and chemical ageing of the membrane could be collectively accessed. In addition, the home-design membrane testing cells can also be used to conduct the fatigue test of water treatment membranes by changing the flow direction at low frequencies. Using the continuous recorded pressure (strength) — deflection behaviors, the microstructure evolution of the membranes can be studied. Moreover, environmental effects can also be coupled with the home designed membrane testing cells to study the fatigue properties of the membrane.

5.3. Real-time micromechanical investigations

As discussed in Section 3.3, the mechanical behaviors of membranes are highly dependent on pore morphology, pore size distribution and microstructure. In order to study the mechanical integrity of nanoporous graphene as desalination membrane, Cohen-Tanugi and Grossman [14] conducted a molecular dynamic simulation. In their simulation, the pore size increased with increasing bi-axial strain with the stress concentration around the nanopores. The

26

failure in nanoporous graphene was characterized by a brittle manner initiated at the nanopores starting from a nucleated defect. Although the simulation was well conducted to predict the physique and mechanical properties of the desalination membranes, laboratory in-situ experiments would eventually be able to characterize the mechanical behavior of these membranes with underlying mechanisms for next generation desalination membranes [14].

In addition, not only the mechanical deformation can results in membrane microstructure evolution, cleaning and ageing effect can also lead to the change of the membrane microstructure affecting flux and permeate properties [189] and [190]. Therefore, in-situ/real-time characterization is an effective method to reveal the relationship between the membrane microstructure and its macroscopic behavior. To accomplish that, digital imaging techniques can be a useful tool to study the strain-induced microstructure evolution. At micrometer scale, strain field measurement can be achieved using 2D/3D digital image correlation (DIC) technique. Strain-induced failure initiation and failure propagation can be recorded in a real time manner and correlated to the macroscopic responses of the membranes. In addition, 3D imaging based approaches such as X-ray tomography using both synchrotron and laboratory sources is also potential techniques for studying pore shape evolution, pore orientation, pore size distribution, and neighboring pore interaction during the deformation of the porous membranes[191] and [192]. This technique has been used for imaging and reconstructing the porous structure of water treatment membranes without deformation [193], [194] and [195]. Recently, Viguié et al. [196] used this technique with a resolution of one micron to reconstruct the 3D structure of their hollow fiber membranes. However, the acquisition time was in hour range. In order to investigate the strain-induced (uniaxial and biaxial) microstructure evolution of membranes, it is therefore expected to use an ultrarapid (subsecond time-resolution) X-ray tomography at submicron (nano)-scale. In addition, time resolved X-ray diffraction, including wide-angle X-ray scattering (WAXS) and small-angle X-ray scattering (SAXS) is also an effective technique for investigating the structure–property relationship of materials. WAXS detects chain orientation, orientation-induced crystallization and crystal destruction for polymer samples [197] and SAXS investigate phase structures and cavitation up to ~ 100 nm depending on the wavelength, the sample-to-detector distance and the detector resolution [198] and [199]. Similar to the 3D imaging approaches, the acquisition time, resolution and data treatment technique are the main challenges for the real-time investigations.

6. Conclusions

27

Uniaxial tensile test, bending test, dynamic mechanical analysis, nanoindentation, and bursting tests are the most widely used approaches to investigate the mechanical behaviors of water treatment membranes. In this, most of the studies are conducted at room temperature, the sample geometry, and the loading rate are quite different. Attention has focused on the mechanical properties of the membranes with the effects of processing conditions, the composite composition or filler content. Normal wear, tear and polymer chain breakage induced by fouling and chemical ageing are the main causes of the membrane mechanical degradation. There are very few studies that investigate the underlying deformation mechanisms of water treatment membranes and there are no study that analyzes the difference in the mechanical properties of water treatment membranes when assessed by different testing methods.

The distribution of the shear-stress induced by the flow is non-uniform. The membranes are not only under simple shearing-stress condition induced by laminar flow, but also under complex stress-state induced by turbulence and rotational flow depending on the flow pressure and velocity as well as membrane cell configurations. Therefore, the conventional methods for studying the mechanical properties of the membranes do not represent their actual loading conditions. Advanced mechanical testing techniques should be developed to investigate the membranes under similar stress-state as that experienced in water treatment applications. Home-designed mechanical testing cells are expected to be developed to investigate the mechanical behavior of the membranes under similar loading states.

In addition, it is important to evaluate the temperature and pressure effects on the mechanical responses of the membranes. Moreover, the cyclic pressure condition of the membranes could be simulated by fatigue testing at different frequencies under various environmental conditions. In order to probe the continuous three-dimensional structural changes induced by strain and to correctly analyze the obtained load-deflection behavior, it is required to develop an advanced measurement system. Furthermore, real-time 3D imaging based techniques are potential experimental tools to reveal the relationship of the microstructure evolution–macromechanical property of the membranes. Using rapid, high-resolution, real-time imaging technique, the mechanical behavior of the membranes can be studied with the underlying mechanisms at different scales.

References

[1] G.-d. Kang, Y.-m. Cao
    Development of antifouling reverse osmosis membranes for water treatment: a review

Water Res., 46 (2012), pp. 584–600

[2] M.A. Shannon, P.W. Bohn, M. Elimelech, J.G. Georgiadis, B.J. Marinas, A.M. Mayes
Science and technology for water purification in the coming decades

Nature, 452 (2008), pp. 301–310

[3] M. Elimelech, W.A. Phillip
The future of seawater desalination: energy, technology, and the environment

Science, 333 (2011), pp. 712–717

[4] M.M. Pendergast, E.M.V. Hoek
A review of water treatment membrane nanotechnologies

Energy Environ. Sci., 4 (2011), pp. 1946–1971

[5] N. Misdan, W.J. Lau, A.F. Ismail
Seawater reverse osmosis (SWRO) desalination by thin-film composite membrane—current development, challenges and future prospects

Desalination, 287 (2012), pp. 228–237

[6] B. Nicolaisen
Developments in membrane technology for water treatment

Desalination, 153 (2003), pp. 355–360

[7] H. Huang, K. Schwab, J.G. Jacangelo
Pretreatment for low pressure membranes in water treatment: a review

Environ. Sci. Technol., 43 (2009), pp. 3011–3019

[8] M. Khayet, J.I. Mengual, T. Matsuura
Porous hydrophobic/hydrophilic composite membranes: application in desalination using direct contact membrane distillation

J. Membr. Sci., 252 (2005), pp. 101–113

[9] H. Susanto, M. Ulbricht
Characteristics, performance and stability of polyethersulfone ultrafiltration membranes prepared by phase separation method using different macromolecular additives

J. Membr. Sci., 327 (2009), pp. 125–135

[10] M. Qtaishat, D. Rana, M. Khayet, T. Matsuura

Preparation and characterization of novel hydrophobic/hydrophilic polyetherimide composite membranes for desalination by direct contact membrane distillation

J. Membr. Sci., 327 (2009), pp. 264–273

[11] M. Khayet, T. Matsuura
Application of surface modifying macromolecules for the preparation of membranes for membrane distillation

Desalination, 158 (2003), pp. 51–56

[12] A. Rahimpour, S.S. Madaeni
Polyethersulfone (PES)/cellulose acetate phthalate (CAP) blend ultrafiltration membranes: preparation, morphology, performance and antifouling properties

J. Membr. Sci., 305 (2007), pp. 299–312

[13] V. Vatanpour, S.S. Madaeni, R. Moradian, S. Zinadini, B. Astinchap
Fabrication and characterization of novel antifouling nanofiltration membrane prepared from oxidized multiwalled carbon nanotube/polyethersulfone nanocomposite

J. Membr. Sci., 375 (2011), pp. 284–294

[14] D. Cohen-Tanugi, J.C. Grossman
Mechanical strength of nanoporous graphene as a desalination membrane

Nano Lett., 14 (2014), pp. 6171–6178

[15] D. Cohen-Tanugi, J.C. Grossman
Water desalination across nanoporous graphene

Nano Lett., 12 (2012), pp. 3602–3608

[16] D. Cohen-Tanugi, J.C. Grossman
Nanoporous graphene as a reverse osmosis membrane: recent insights from theory and simulation

Desalination, 366 (2015), pp. 59–70

[17] S. Lin, M.J. Buehler
Mechanics and molecular filtration performance of graphyne nanoweb membranes for selective water purification

Nanoscale, 5 (2013), pp. 11801–11807

30

[18] M. Ding, A. Ghoufi, A. Szymczyk

Molecular simulations of polyamide reverse osmosis membranes

Desalination, 343 (2014), pp. 48–53

[19] T.A. Osswald

Understanding Polymer Processing: Processes and Governing Equations

Hanser Publishers (2011)

[20] H. Zhou, D.W. Smith

Advanced technologies in water and wastewater treatment

J. Environ. Eng. Sci., 1 (2002), pp. 247–264

[21] F. Fu, Q. Wang

Removal of heavy metal ions from wastewaters: a review

J. Environ. Manag., 92 (2011), pp. 407–418

[22] L. Setiawan, R. Wang, K. Li, A.G. Fane

Fabrication of novel poly (amide–imide) forward osmosis hollow fiber membranes with a positively charged nanofiltration-like selective layer

J. Membr. Sci., 369 (2011), pp. 196–205

[23] Y. Zhu, D. Wang, L. Jiang, J. Jin

Recent progress in developing advanced membranes for emulsified oil/water separation

NPG Asia Mater., 6 (2014), Article e101

[24] J. Kim, B. Van der Bruggen

The use of nanoparticles in polymeric and ceramic membrane structures: review of manufacturing procedures and performance improvement for water treatment

Environ. Pollut., 158 (2010), pp. 2335–2349

[25] M.G. Buonomenna

Nano-enhanced reverse osmosis membranes

Desalination, 314 (2013), pp. 73–88

[26] K.A. Mahmoud, B. Mansoor, A. Mansour, M. Khraisheh

Functional graphene nanosheets: the next generation membranes for water desalination

Desalination, 356 (2015), pp. 208–225

31

[27] A. ElMekawy, H.M. Hegab, D. Pant

The near-future integration of microbial desalination cells with reverse osmosis technology

Energy Environ. Sci. (2014)

[28] G.K. Pearce

UF/MF Membrane Water Treatment: Principles and Design

Water Treatment Academy Bangkok (2011)

[29] R.P. Vinci, J.J. Vlassak

Mechanical behavior of thin films

Annu. Rev. Mater. Sci., 26 (1996), pp. 431–462

[30]

S.V. Kamat

Experimental techniques for the measurement of mechanical properties of materials used in microelectromechanical systems

Def. Sci. J., 59 (2009), pp. 605–615

[31] H. Espinosa, B. Prorok

Size effects on the mechanical behavior of gold thin films

J. Mater. Sci., 38 (2003), pp. 4125–4128

[32] X. Zhang, C. Xiao, X. Hu, Q. Bai

Preparation and properties of homogeneous-reinforced polyvinylidene fluoride hollow fiber membrane

Appl. Surf. Sci., 264 (2013), pp. 801–810

[33] X. Zhu, H.-E. Loo, R. Bai

A novel membrane showing both hydrophilic and oleophobic surface properties and its non-fouling performances for potential water treatment applications

J. Membr. Sci., 436 (2013), pp. 47–56

[34] Y.-j. Wu, Q.-l. Huang, C.-f. Xiao, K.-k. Chen, X.-f. Li, N.-n. Li

Study on the effects and properties of PVDF/FEP blend porous membrane

Desalination, 353 (2014), pp. 118–124

[35] D. Hou, J. Wang, X. Sun, Z. Ji, Z. Luan

Preparation and properties of PVDF composite hollow fiber membranes for desalination through direct contact membrane distillation

J. Membr. Sci., 405 (2012), pp. 185–200

[36] C.Y. Lai, A. Groth, S. Gray, M. Duke

Enhanced abrasion resistant PVDF/nanoclay hollow fibre composite membranes for water treatment

J. Membr. Sci., 449 (2014), pp. 146–157

[37] A. Cui, Z. Liu, C. Xiao, Y. Zhang

Effect of micro-sized SiO_2-particle on the performance of PVDF blend membranes via TIPS
J. Membr. Sci., 360 (2010), pp. 259–264

[38] L.-Y. Yu, Z.-L. Xu, H.-M. Shen, H. Yang

Preparation and characterization of PVDF–SiO_2 composite hollow fiber UF membrane by sol–gel method
J. Membr. Sci., 337 (2009), pp. 257–265

[39] J. Hong, Y. He

Effects of nano sized zinc oxide on the performance of PVDF microfiltration membranes

Desalination, 302 (2012), pp. 71–79

[40] P. Sukitpaneenit, T.-S. Chung

Molecular elucidation of morphology and mechanical properties of PVDF hollow fiber membranes from aspects of phase inversion, crystallization and rheology

J. Membr. Sci., 340 (2009), pp. 192–205

[41] B.J. Cha, J.M. Yang

Preparation of poly(vinylidene fluoride) hollow fiber membranes for microfiltration using modified TIPS process

J. Membr. Sci., 291 (2007), pp. 191–198

[42] S. Simone, A. Figoli, A. Criscuoli, M.C. Carnevale, A. Rosselli, E. Drioli
Preparation of hollow fibre membranes from PVDF/PVP blends and their application in VMD

J. Membr. Sci., 364 (2010), pp. 219–232

[43] D.-J. Lin, C.-L. Chang, C.-K. Lee, L.-P. Cheng

Preparation and characterization of microporous PVDF/PMMA composite membranes by phase inversion in water/DMSO solutions

Eur. Polym. J., 42 (2006), pp. 2407–2418

[44] L. Yan, Y.S. Li, C.B. Xiang

Preparation of poly(vinylidene fluoride) (PVDF) ultrafiltration membrane modified by nano-sized alumina (Al_2O_3) and its antifouling research
Polymer, 46 (2005), pp. 7701–7706

[45] L. Yan, Y.S. Li, C.B. Xiang, S. Xianda
Effect of nano-sized Al_2O_3-particle addition on PVDF ultrafiltration membrane performance
J. Membr. Sci., 276 (2006), pp. 162–167

[46] N.-N. Bui, J.R. McCutcheon
Hydrophilic nanofibers as new supports for thin film composite membranes for engineered osmosis

Environ. Sci. Technol., 47 (2013), pp. 1761–1769

[47] S. Zhang, F. Fu, T.-S. Chung
Substrate modifications and alcohol treatment on thin film composite membranes for osmotic power

Chem. Eng. Sci., 87 (2013), pp. 40–50

[48] A. Ahmad, S. Waheed, S.M. Khan, S. e-Gul, M. Shafiq, M. Farooq, K. Sanaullah, T. Jamil
Effect of silica on the properties of cellulose acetate/polyethylene glycol membranes for reverse osmosis

Desalination, 355 (2015), pp. 1–10

[49] R. Wang, L. Shi, C.Y. Tang, S. Chou, C. Qiu, A.G. Fane
Characterization of novel forward osmosis hollow fiber membranes

J. Membr. Sci., 355 (2010), pp. 158–167

[50] J. Qin, T.-S. Chung
Effect of dope flow rate on the morphology, separation performance, thermal and mechanical properties of ultrafiltration hollow fibre membranes

J. Membr. Sci., 157 (1999), pp. 35–51

34

[51] E.M.V. Hoek, A.K. Ghosh, X. Huang, M. Liong, J.I. Zink
Physical–chemical properties, separation performance, and fouling resistance of mixed-matrix ultrafiltration membranes

Desalination, 283 (2011), pp. 89–99

[52] W. Fang, L. Shi, R. Wang
Interfacially polymerized composite nanofiltration hollow fiber membranes for low-pressure water softening

J. Membr. Sci., 430 (2013), pp. 129–139

[53] A. Razmjou, A. Resosudarmo, R.L. Holmes, H. Li, J. Mansouri, V. Chen
The effect of modified TiO_2 nanoparticles on the polyethersulfone ultrafiltration hollow fiber membranes
Desalination, 287 (2012), pp. 271–280

[54] Y. Ma, F. Shi, Z. Wang, M. Wu, J. Ma, C. Gao
Preparation and characterization of PSf/clay nanocomposite membranes with PEG 400 as a pore forming additive

Desalination, 286 (2012), pp. 131–137

[55] Z. Fan, Z. Wang, N. Sun, J. Wang, S. Wang
Performance improvement of polysulfone ultrafiltration membrane by blending with polyaniline nanofibers

J. Membr. Sci., 320 (2008), pp. 363–371

[56] L. Brunet, D.Y. Lyon, K. Zodrow, J.C. Rouch, B. Caussat, P. Serp, J.C. Remigy, M.R. Wiesner, P.J.J. Alvarez
Properties of membranes containing semi-dispersed carbon nanotubes

Environ. Eng. Sci., 25 (2008), pp. 565–576

[57] J. Lee, H.-R. Chae, Y.J. Won, K. Lee, C.-H. Lee, H.H. Lee, I.-C. Kim, J.-m. Lee
Graphene oxide nanoplatelets composite membrane with hydrophilic and antifouling properties for wastewater treatment

J. Membr. Sci., 448 (2013), pp. 223–230

[58] S. Maphutha, K. Moothi, M. Meyyappan, S.E. Iyuke

A carbon nanotube-infused polysulfone membrane with polyvinyl alcohol layer for treating oil-containing waste water

Sci. Rep., 3 (2013)

[59] G. Han, T.-S. Chung, M. Toriida, S. Tamai
Thin-film composite forward osmosis membranes with novel hydrophilic supports for desalination

J. Membr. Sci., 423–424 (2012), pp. 543–555

[60] X. Wang, D. Fang, K. Yoon, B.S. Hsiao, B. Chu
High performance ultrafiltration composite membranes based on poly(vinyl alcohol) hydrogel coating on crosslinked nanofibrous poly(vinyl alcohol) scaffold

J. Membr. Sci., 278 (2006), pp. 261–268

[61] X. Li, Y. Zhang, H. Li, H. Chen, Y. Ding, W. Yang
Effect of oriented fiber membrane fabricated via needleless melt electrospinning on water filtration efficiency

Desalination, 344 (2014), pp. 266–273

[62] B. Bae, B.H. Chun, D. Kim
Surface characterization of microporous polypropylene membranes modified by plasma treatment

Polymer, 42 (2001), pp. 7879–7885

[63] H.-Y. Yu, Y.-J. Xie, M.-X. Hu, J.-L. Wang, S.-Y. Wang, Z.-K. Xu
Surface modification of polypropylene microporous membrane to improve its antifouling property in MBR: CO_2 plasma treatment
J. Membr. Sci., 254 (2005), pp. 219–227

[64] A.G. Boricha, Z.V.P. Murthy
Preparation of *N*,*O*-carboxymethyl chitosan/cellulose acetate blend nanofiltration membrane and testing its performance in treating industrial wastewater
Chem. Eng. J., 157 (2010), pp. 393–400

[65] C. Tang, Q. Zhang, K. Wang, Q. Fu, C. Zhang
Water transport behavior of chitosan porous membranes containing multi-walled carbon nanotubes (MWNTs)

J. Membr. Sci., 337 (2009), pp. 240–247

[66] A. Kritikaki, A. Tsetsekou

Fabrication of porous alumina ceramics from powder mixtures with sol–gel derived nanometer alumina: effect of mixing method

J. Eur. Ceram. Soc., 29 (2009), pp. 1603–1611

[67] Y. Wang, Y. Zhang, X. Liu, G. Meng

Sol-coated preparation and characterization of macroporous α-Al_2O_3 membrane support

J. Sol-Gel Sci. Technol., 41 (2007), pp. 267–275

[68] Z.Y. Deng, T. Fukasawa, M. Ando, G.J. Zhang, T. Ohji

Microstructure and mechanical properties of porous alumina ceramics fabricated by the decomposition of aluminum hydroxide

J. Am. Ceram. Soc., 84 (2001), pp. 2638–2644

[69] S. Sarkar, S. Bandyopadhyay, A. Larbot, S. Cerneaux

New clay–alumina porous capillary supports for filtration application

J. Membr. Sci., 392–393 (2012), pp. 130–136

[70] H. Qi, Y. Fan, W. Xing, L. Winnubst

Effect of TiO_2 doping on the characteristics of macroporous Al_2O_3/TiO_2 membrane supports

J. Eur. Ceram. Soc., 30 (2010), pp. 1317–1325

[71] B.K. Nandi, R. Uppaluri, M.K. Purkait

Preparation and characterization of low cost ceramic membranes for micro-filtration applications

Appl. Clay Sci., 42 (2008), pp. 102–110

[72] D. Vasanth, G. Pugazhenthi, R. Uppaluri

Fabrication and properties of low cost ceramic microfiltration membranes for separation of oil and bacteria from its solution

J. Membr. Sci., 379 (2011), pp. 154–163

[73] D. Vasanth, G. Pugazhenthi, R. Uppaluri

Cross-flow microfiltration of oil-in-water emulsions using low cost ceramic membranes

Desalination, 320 (2013), pp. 86–95

37

[74] P. Monash, G. Pugazhenthi

Effect of TiO_2 addition on the fabrication of ceramic membrane supports: a study on the separation of oil droplets and bovine serum albumin (BSA) from its solution

Desalination, 279 (2011), pp. 104–114

[75] P. Monash, G. Pugazhenthi

Development of ceramic supports derived from low-cost raw materials for membrane applications and its optimization based on sintering temperature

Int. J. Appl. Ceram. Technol., 8 (2011), pp. 227–238

[76] S.-M. Lee, I.-H. Choi, S.-W. Myung, J.-y. Park, I.-C. Kim, W.-N. Kim, K.-H. Lee
Preparation and characterization of nickel hollow fiber membrane

Desalination, 233 (2008), pp. 32–39

[77] S. Kroll, L. Treccani, K. Rezwan, G. Grathwohl
Development and characterisation of functionalised ceramic microtubes for bacteria filtration

J. Membr. Sci., 365 (2010), pp. 447–455

[78] T.-S. Chung, J.-J. Qin, J. Gu
Effect of shear rate within the spinneret on morphology, separation performance and mechanical properties of ultrafiltration polyethersulfone hollow fiber membranes

Chem. Eng. Sci., 55 (2000), pp. 1077–1091

[79] T.-Y. Liu, R.-X. Zhang, Q. Li, B. Van der Bruggen, X.-L. Wang
Fabrication of a novel dual-layer (PES/PVDF) hollow fiber ultrafiltration membrane for wastewater treatment

J. Membr. Sci., 472 (2014), pp. 119–132

[80] S.S. Homaeigohar, M. Elbahri
Novel compaction resistant and ductile nanocomposite nanofibrous microfiltration membranes

J. Colloid Interface Sci., 372 (2012), pp. 6–15

[81] S. Singh, P. Patel, V.K. Shahi, U. Chudasama
Pb^{2+} selective and highly cross-linked zirconium phosphonate membrane by sol–gel in aqueous media for electrochemical applications

38

Desalination, 276 (2011), pp. 175–183

[82] A.K. Singh, A.K. Thakur, V.K. Shahi

Self-assembled nanofiltration membrane containing antimicrobial organosilica prepared by sol–gel process

Desalination, 309 (2013), pp. 275–283

[83] X. Zhang, C. Xiao, X. Hu, X. Jin, Q. Bai
Study on the interfacial bonding state and fouling phenomena of polyvinylidene fluoride matrix-reinforced hollow fiber membranes during microfiltration

Desalination, 330 (2013), pp. 49–60

[84] F. Kayaci, Z. Aytac, T. Uyar
Surface modification of electrospun polyester nanofibers with cyclodextrin polymer for the removal of phenanthrene from aqueous solution

J. Hazard. Mater., 261 (2013), pp. 286–294

[85] S. Gahlot, P.P. Sharma, H. Gupta, V. Kulshrestha, P.K. Jha
Preparation of graphene oxide nano-composite ion-exchange membranes for desalination application

RSC Adv., 4 (2014), pp. 24662–24670

[86] V. Saucedo-Rivalcoba, A.L. Martínez-Hernández, G. Martínez-Barrera, C. Velasco-Santos, J.L. Rivera-Armenta, V.M. Castaño
Removal of hexavalent chromium from water by polyurethane–keratin hybrid membranes, water, air

Soil Pollut., 218 (2011), pp. 557–571

[87] I. Yakub
Micro- and Nano-Porous Adsorptive Materials for Removal of Contaminants from Water at Point-of-Use

Princeton University (2012)

[88] S. Homaeigohar, J. Koll, E.T. Lilleodden, M. Elbahri
The solvent induced interfiber adhesion and its influence on the mechanical and filtration properties of polyethersulfone electrospun nanofibrous microfiltration membranes

Sep. Purif. Technol., 98 (2012), pp. 456–463

[89] J. Yeo, S.Y. Kim, S. Kim, D.Y. Ryu, T.H. Kim, M.J. Park
Mechanically and structurally robust sulfonated block copolymer membranes for water purification applications

Nanotechnology, 23 (2012), p. 245703

[90] N. Wang, S. Ji, G. Zhang, J. Li, L. Wang
Self-assembly of graphene oxide and polyelectrolyte complex nanohybrid membranes for nanofiltration and pervaporation

Chem. Eng. J., 213 (2012), pp. 318–329

[91] M.H. Tai, P. Gao, B.Y.L. Tan, D.D. Sun, J.O. Leckie
Highly efficient and flexible electrospun carbon–silica nanofibrous membrane for ultrafast gravity-driven oil–water separation

ACS Appl. Mater. Interfaces, 6 (2014), pp. 9393–9401

[92] H. Wang, T.-S. Chung, Y.W. Tong, W. Meier, Z. Chen, M. Hong, K. Jeyaseelan, A. Armugam

Preparation and characterization of pore-suspending biomimetic membranes embedded with Aquaporin Z on carboxylated polyethylene glycol polymer cushion

Soft Matter, 7 (2011), pp. 7274–7280

[93] P. Wang, T.-S. Chung
A new-generation asymmetric multi-bore hollow fiber membrane for sustainable water production via vacuum membrane distillation

Environ. Sci. Technol., 47 (2013), pp. 6272–6278

[94] N. Li, C. Xiao, S. An, X. Hu
Preparation and properties of PVDF/PVA hollow fiber membranes

Desalination, 250 (2010), pp. 530–537

[95] B.S. Lalia, E. Guillen-Burrieza, H.A. Arafat, R. Hashaikeh
Fabrication and characterization of polyvinylidenefluoride-*co*-hexafluoropropylene (PVDF-HFP) electrospun membranes for direct contact membrane distillation
J. Membr. Sci., 428 (2013), pp. 104–115

[96] J. Liu, P. Li, Y. Li, L. Xie, S. Wang, Z. Wang
Preparation of PET threads reinforced PVDF hollow fiber membrane
Desalination, 249 (2009), pp. 453–457

[97] S. Chou, R. Wang, L. Shi, Q. She, C. Tang, A.G. Fane
Thin-film composite hollow fiber membranes for pressure retarded osmosis (PRO) process with high power density
J. Membr. Sci., 389 (2012), pp. 25–33

[98] N. Tanaka, M. Nagase, M. Higa
Organic fouling behavior of anion exchange membranes prepared from chloromethyl styrene and divinylbenzene
Desalin. Water Treat., 17 (2010), pp. 248–254

[99] L. Li, R. Hashaikeh, H.A. Arafat
Development of eco-efficient micro-porous membranes via electrospinning and annealing of poly(lactic acid)
J. Membr. Sci., 436 (2013), pp. 57–67

[100] Y. Yang, H. Zhang, P. Wang, Q. Zheng, J. Li
The influence of nano-sized TiO_2 fillers on the morphologies and properties of PSF UF membrane
J. Membr. Sci., 288 (2007), pp. 231–238

[101] S. Chou, R. Wang, A.G. Fane
Robust and high performance hollow fiber membranes for energy harvesting from salinity gradients by pressure retarded osmosis
J. Membr. Sci., 448 (2013), pp. 44–54

[102] K. Wang, F. Addiego, N. Bahlouli, S. Ahzi, Y. Rémond, V. Toniazzo, R. Muller
Analysis of thermomechanical reprocessing effects on polypropylene/ethylene octene copolymer blends
Polym. Degrad. Stab., 97 (2012), pp. 1475–1484

[103] K. Wang, N. Bahlouli, F. Addiego, S. Ahzi, Y. Rémond, D. Ruch, R. Muller
Effect of talc content on the degradation of re-extruded polypropylene/talc composites
Polym. Degrad. Stab., 98 (2013), pp. 1275–1286

41

[104] K. Wang, F. Addiego, A. Laachachi, B. Kaouache, N. Bahlouli, V. Toniazzo, D. Ruch

Dynamic behavior and flame retardancy of HDPE/hemp short fiber composites: effect of coupling agent and fiber loading

Compos. Struct., 113 (2014), pp. 74–82

[105] A. Upitis, J. Peterson, C. Lukey, L.D. Nghiem
Metallic ion extraction using polymer inclusion membranes (PIMs): optimising physical strength and extraction rate

Desalin. Water Treat., 6 (2009), pp. 41–47

[106] F.V. Adams, E.N. Nxumalo, R.W.M. Krause, E.M.V. Hoek, B.B. Mamba
Preparation and characterization of polysulfone/β-cyclodextrin polyurethane composite nanofiltration membranes

J. Membr. Sci., 405–406 (2012), pp. 291–299

[107] E. Gaudichet-Maurin, F. Thominette
Ageing of polysulfone ultrafiltration membranes in contact with bleach solutions

J. Membr. Sci., 282 (2006), pp. 198–204

[108] M.-C. Yang, T.-Y. Liu
The permeation performance of polyacrylonitrile/polyvinylidine fluoride blend membranes

J. Membr. Sci., 226 (2003), pp. 119–130

[109] J. Wang, W.-Z. Lang, H.-P. Xu, X. Zhang, Y.-J. Guo
Improved poly(vinyl butyral) hollow fiber membranes by embedding multi-walled carbon nanotube for the ultrafiltrations of bovine serum albumin and humic acid

Chem. Eng. J., 260 (2015), pp. 90–98

[110] F. Ejaz Ahmed, B.S. Lalia, N. Hilal, R. Hashaikeh
Underwater superoleophobic cellulose/electrospun PVDF–HFP membranes for efficient oil/water separation

Desalination, 344 (2014), pp. 48–54

[111] Z. Wang, H. Yu, J. Xia, F. Zhang, F. Li, Y. Xia, Y. Li
Novel GO-blended PVDF ultrafiltration membranes

Desalination, 299 (2012), pp. 50–54

[112] G. Han, S. Zhang, X. Li, T.-S. Chung

High performance thin film composite pressure retarded osmosis (PRO) membranes for renewable salinity-gradient energy generation

J. Membr. Sci., 440 (2013), pp. 108–121

[113] Y. Ma, F. Shi, J. Ma, M. Wu, J. Zhang, C. Gao
Effect of PEG additive on the morphology and performance of polysulfone ultrafiltration membranes

Desalination, 272 (2011), pp. 51–58

[114] A. Bazargan, M. Keyanpour-Rad, F. Hesari, M.E. Ganji
A study on the microfiltration behavior of self-supporting electrospun nanofibrous membrane in water using an optical particle counter

Desalination, 265 (2011), pp. 148–152

[115] J. Liu, X. Lu, J. Li, C. Wu
Preparation and properties of poly(vinylidene fluoride) membranes via the low temperature thermally induced phase separation method

J. Polym. Res., 21 (2014), pp. 1–16

[116] N. Widjojo, T.-S. Chung, M. Weber, C. Maletzko, V. Warzelhan
The role of sulphonated polymer and macrovoid-free structure in the support layer for thin-film composite (TFC) forward osmosis (FO) membranes

J. Membr. Sci., 383 (2011), pp. 214–223

[117] H.A. Shawky, S.-R. Chae, S. Lin, M.R. Wiesner
Synthesis and characterization of a carbon nanotube/polymer nanocomposite membrane for water treatment

Desalination, 272 (2011), pp. 46–50

[118] K. Yoon, B.S. Hsiao, B. Chu
Formation of functional polyethersulfone electrospun membrane for water purification by mixed solvent and oxidation processes

Polymer, 50 (2009), pp. 2893–2899

[119] H. Ma, K. Yoon, L. Rong, Y. Mao, Z. Mo, D. Fang, Z. Hollander, J. Gaiteri, B.S. Hsiao, B. Chu

43

High-flux thin-film nanofibrous composite ultrafiltration membranes containing cellulose barrier layer

J. Mater. Chem., 20 (2010), pp. 4692–4704

[120] A.E. Childress, P. Le-Clech, J.L. Daugherty, C. Chen, G.L. Leslie
Mechanical analysis of hollow fiber membrane integrity in water reuse applications

Desalination, 180 (2005), pp. 5–14

[121] S. Liu, K. Li, R. Hughes
Preparation of porous aluminium oxide (Al_2O_3) hollow fibre membranes by a combined phase-inversion and sintering method
Ceram. Int., 29 (2003), pp. 875–881

[122] M.W. Luiten-Olieman, L. Winnubst, A. Nijmeijer, M. Wessling, N.E. Benes
Porous stainless steel hollow fiber membranes via dry–wet spinning

J. Membr. Sci., 370 (2011), pp. 124–130

[123] A.F. Bower
Applied Mechanics of Solids

CRC press (2009)

[124] R.P. Chartoff, J.D. Menczel, S.H. Dillman
Dynamic mechanical analysis (DMA)

Thermal Analysis of Polymers, John Wiley & Sons, Inc. (2008), pp. 387–495

[125] C.A. Schuh
Nanoindentation studies of materials

Mater. Today, 9 (2006), pp. 32–40

[126] G.M. Pharr
Measurement of mechanical properties by ultra-low load indentation

Mater. Sci. Eng. A Struct., 253 (1998), pp. 151–159

[127] M.R. VanLandingham
Review of instrumented indentation

J. Res. Natl. Inst. Stand. Technol., 108 (2003), pp. 249–265

[128] M.F. Doerner, W.D. Nix

A method for interpreting the data from depth-sensing indentation instruments

J. Mater. Res., 1 (1986), pp. 601–609

[129] W.C. Oliver, G.M. Pharr
An improved technique for determining hardness and elastic modulus using load and displacement sensing indentation experiments

J. Mater. Res., 7 (1992), pp. 1564–1583

[130] D. Johnson, N. Hilal
Characterisation and quantification of membrane surface properties using atomic force microscopy: a comprehensive review

Desalination, 356 (2015), pp. 149–164

[131] J. Malohlava, H. Zapletalova, K. Tomankova, H. Kolarova
Atomic Force Microscopy: Studying Mechanical Properties of a Cell

(2012)

[132] C. Plassard, E. Lesniewska, I. Pochard, A. Nonat
Investigation of the surface structure and elastic properties of calcium silicate hydrates at the nanoscale

Ultramicroscopy, 100 (2004), pp. 331–338

[133] B. Kracke, B. Damaschke
Measurement of nanohardness and nanoelasticity of thin gold films with scanning force microscope

Appl. Phys. Lett., 77 (2000), pp. 361–363

[134] M. Jaroslav
Uncertainties and errors in nanoindentation

J. Nemecek (Ed.), Nanoindentation in Materials Science, InTech (2012)

[135] P.V. Vyas, P. Ray, S.K. Adhikary, B.G. Shah, R. Rangarajan
Studies of the effect of variation of blend ratio on permselectivity and heterogeneity of ion-exchange membranes

J. Colloid Interface Sci., 257 (2003), pp. 127–134

[136] V. Bhardwaj, A. Macintosh, I.D. Sharpe, S.A. Gordeyev, S.J. Shilton

Polysulfone hollow fiber gas separation membranes filled with submicron particles

Ann. N. Y. Acad. Sci., 984 (2003), pp. 318–328

[137] N. Tanaka, M. Nagase, M. Higa
Preparation of aliphatic-hydrocarbon-based anion-exchange membranes and their anti-organic-fouling properties

J. Membr. Sci., 384 (2011), pp. 27–36

[138] C. Zhou, Z. Hou, X. Lu, Z. Liu, X. Bian, L. Shi, L. Li
Effect of polyethersulfone molecular weight on structure and performance of ultrafiltration membranes

Ind. Eng. Chem. Res., 49 (2010), pp. 9988–9997

[139] S. Zhang, P. Sukitpaneenit, T.-S. Chung
Design of robust hollow fiber membranes with high power density for osmotic energy production

Chem. Eng. J., 241 (2014), pp. 457–465

[140] S. Zhang, T.-S. Chung
Minimizing the instant and accumulative effects of salt permeability to sustain ultrahigh osmotic power density

Environ. Sci. Technol., 47 (2013), pp. 10085–10092

[141] M.K. Khraisheh, H.M. Zbib
Optimum forming loading paths for Pb–Sn superplastic sheet materials

J. Eng. Mater. Technol., 121 (1999), pp. 341–345

[142] S.P. Chesters, N. Pena, S. Gallego, M. Fazel, M.W. Armstrong, F. del Vigo
Results from 99 seawater RO membrane autopsies

IDA J. Desalin. Water Reuse, 5 (2013), pp. 40–47

[143] A. Gijsbertsen-Abrahamse, E. Cornelissen, J. Hofman
Fiber failure frequency and causes of hollow fiber integrity loss

Desalination, 194 (2006), pp. 251–258

[144] E. Zondervan, A. Zwijnenburg, B. Roffel
Statistical analysis of data from accelerated ageing tests of PES UF membranes

J. Membr. Sci., 300 (2007), pp. 111–116

[145] H. Guo, Y. Wyart, J. Perot, F. Nauleau, P. Moulin
Low-pressure membrane integrity tests for drinking water treatment: a review

Water Res., 44 (2010), pp. 41–57

[146] N. Peña, S. Gallego, F. Del Vigo, S. Chesters
Evaluating impact of fouling on reverse osmosis membranes performance

Desalin. Water Treat., 51 (2013), pp. 958–968

[147] D.M. Warsinger, J. Swaminathan, E. Guillen-Burrieza, H.A. Arafat, J.H. Lienhard V
Scaling and fouling in membrane distillation for desalination applications: a review

Desalination, 356 (2015), pp. 294–313

[148] Y. He, J. Sharma, R. Bogati, B. Liao, C. Goodwin, K. Marshall
Impacts of aging and chemical cleaning on the properties and performance of ultrafiltration
membranes in potable water treatment

Sep. Sci. Technol., 49 (2014), pp. 1317–1325

[149] V. Kochkodan, N. Hilal
o   A comprehensive review on surface modified polymer membranes for biofouling mitigation

o   Desalination, 356 (2015), pp. 187–207

[150] M. Gryta
Desalination of Industrial Effluents Using Integrated Membrane Processes

INTECH Open Access Publisher (2012)

[151] L.D. Nghiem, A.I. Schäfer
Fouling autopsy of hollow-fibre MF membranes in wastewater reclamation

Desalination, 188 (2006), pp. 113–121

[152] N. Porcelli, S. Judd
Chemical cleaning of potable water membranes: a review

Sep. Purif. Technol., 71 (2010), pp. 137–143

[153] M.G. Khedr
Development of reverse osmosis desalination membranes composition and configuration:
future prospects

47

Desalination, 153 (2003), pp. 295–304

[154] M.J. Cran, S.W. Bigger, S.R. Gray

Degradation of polyamide reverse osmosis membranes in the presence of chloramine

Desalination, 283 (2011), pp. 58–63

[155] B. Pellegrin, R. Prulho, A. Rivaton, S. Thérias, J.-L. Gardette, E. Gaudichet-Maurin, C. Causserand

Multi-scale analysis of hypochlorite induced PES/PVP ultrafiltration membranes degradation

J. Membr. Sci., 447 (2013), pp. 287–296

[156] P. Cote, Z. Alam, J. Penny

Hollow fiber membrane life in membrane bioreactors (MBR)

Desalination, 288 (2012), pp. 145–151

[157] E. Arkhangelsky, D. Kuzmenko, N.V. Gitis, M. Vinogradov, S. Kuiry, V. Gitis

Hypochlorite cleaning causes degradation of polymer membranes

Tribol. Lett., 28 (2007), pp. 109–116

[158] E. Arkhangelsky, U. Goren, V. Gitis

Retention of organic matter by cellulose acetate membranes cleaned with hypochlorite

Desalination, 223 (2008), pp. 97–105

[159] C. Causserand, S. Rouaix, J.-P. Lafaille, P. Aimar

Ageing of polysulfone membranes in contact with bleach solution: role of radical oxidation and of some dissolved metal ions

Chem. Eng. Process., 47 (2008), pp. 48–56

[160] S. Rouaix, C. Causserand, P. Aimar

Experimental study of the effects of hypochlorite on polysulfone membrane properties

J. Membr. Sci., 277 (2006), pp. 137–147

[161] G.D. Vilakati, M.C. Wong, E.M. Hoek, B.B. Mamba

Relating thin film composite membrane performance to support membrane morphology fabricated using lignin additive

J. Membr. Sci., 469 (2014), pp. 216–224

[162] F.-J. Fu, S. Zhang, S.-P. Sun, K.-Y. Wang, T.-S. Chung

POSS-containing delamination-free dual-layer hollow fiber membranes for forward osmosis and osmotic power generation

J. Membr. Sci., 443 (2013), pp. 144–155

[163] R. Revanur, B. McCloskey, K. Breitenkamp, B.D. Freeman, T. Emrick

Reactive amphiphilic graft copolymer coatings applied to poly (vinylidene fluoride) ultrafiltration membranes

Macromolecules, 40 (2007), pp. 3624–3630

[164] S.P. Sun, K.Y. Wang, N. Peng, T.A. Hatton, T.-S. Chung
Novel polyamide–imide/cellulose acetate dual-layer hollow fiber membranes for nanofiltration

J. Membr. Sci., 363 (2010), pp. 232–242

[165] N. Widjojo, T.S. Chung, W.B. Krantz
A morphological and structural study of Ultem/P84 copolyimide dual-layer hollow fiber membranes with delamination-free morphology

J. Membr. Sci., 294 (2007), pp. 132–146

[166] L.A. Hoover, J.D. Schiffman, M. Elimelech
Nanofibers in thin-film composite membrane support layers: enabling expanded application of forward and pressure retarded osmosis

Desalination, 308 (2013), pp. 73–81

[167] Q. She, D. Hou, J. Liu, K.H. Tan, C.Y. Tang
Effect of feed spacer induced membrane deformation on the performance of pressure retarded osmosis (PRO): implications for PRO process operation

J. Membr. Sci., 445 (2013), pp. 170–182

[168] Y.C. Kim, M. Elimelech
Adverse impact of feed channel spacers on the performance of pressure retarded osmosis

Environ. Sci. Technol., 46 (2012), pp. 4673–4681

[169] F. Cortés-Juan, B. Balannec, T. Renouard
CFD-assisted design improvement of a bench-scale nanofiltration cell

Sep. Purif. Technol., 82 (2011), pp. 177–184

[170] S.S. Sablani, M.F. Goosen, R. Al-Belushi, V. Gerardos
Influence of spacer thickness on permeate flux in spiral-wound seawater reverse osmosis systems

Desalination, 146 (2002), pp. 225–230

[171] J. Schwinge, D. Wiley, D. Fletcher
A CFD study of unsteady flow in narrow spacer-filled channels for spiral-wound membrane modules

Desalination, 146 (2002), pp. 195–201

[172] J. Santos, V. Geraldes, S. Velizarov, J. Crespo
Investigation of flow patterns and mass transfer in membrane module channels filled with flow-aligned spacers using computational fluid dynamics (CFD)

J. Membr. Sci., 305 (2007), pp. 103–117

[173] V.t. Geraldes, V. Semião, M.N. de Pinho
Flow management in nanofiltration spiral wound modules with ladder-type spacers

J. Membr. Sci., 203 (2002), pp. 87–102

[174] C. Koutsou, S. Yiantsios, A. Karabelas
Numerical simulation of the flow in a plane-channel containing a periodic array of cylindrical turbulence promoters

J. Membr. Sci., 231 (2004), pp. 81–90

[175] C. Koutsou, S. Yiantsios, A. Karabelas
Direct numerical simulation of flow in spacer-filled channels: effect of spacer geometrical characteristics

J. Membr. Sci., 291 (2007), pp. 53–69

[176] R. Kaya, G. Deveci, T. Turken, R. Sengur, S. Guclu, D.Y. Koseoglu-Imer, I. Koyuncu
Analysis of wall shear stress on the outside-in type hollow fiber membrane modules by CFD simulation

Desalination, 351 (2014), pp. 109–119

[177] K. Wang, F. Addiego, N. Bahlouli, S. Ahzi, Y. Rémond, V. Toniazzo

50

Impact response of recycled polypropylene-based composites under a wide range of temperature: effect of filler content and recycling

Compos. Sci. Technol., 95 (2014), pp. 89–99

[178] K. Wang, S. Ahzi, R. Matadi Boumbimba, N. Bahlouli, F. Addiego, Y. Rémond
Micromechanical modeling of the elastic behavior of polypropylene based organoclay nanocomposites under a wide range of temperatures and strain rates/frequencies

Mech. Mater., 64 (2013), pp. 56–68

[179] K. Wang, R.M. Boumbimba, N. Bahlouli, S. Ahzi, R. Muller, M. Bouquey
Dynamic behaviour of a melt mixing polypropylene organoclay nanocomposites

J. Eng. Mater. Technol., 134 (2012), p. 010905

[180] B.M. Darras, M. Omar, M.K. Khraisheh
Experimental thermal analysis of friction stir processing

MSF, Trans Tech Publ (2007), pp. 3801–3806

[181] B. Andrews, B. Davé, P. López-Serrano, S.-P. Tsai, R. Frank, M. Wilf, E. Koutsakos
Effective scale control for seawater RO operating with high feed water pH and temperature

Desalination, 220 (2008), pp. 295–304

[182] X. Jin, A. Jawor, S. Kim, E.M.V. Hoek
Effects of feed water temperature on separation performance and organic fouling of brackish water RO membranes

Desalination, 239 (2009), pp. 346–359

[183] A. Antony, J.H. Low, S. Gray, A.E. Childress, P. Le-Clech, G. Leslie
Scale formation and control in high pressure membrane water treatment systems: a review

J. Membr. Sci., 383 (2011), pp. 1–16

[184] H. Mo, K.G. Tay, H.Y. Ng
Fouling of reverse osmosis membrane by protein (BSA): effects of pH, calcium, magnesium, ionic strength and temperature

J. Membr. Sci., 315 (2008), pp. 28–35

[185] M.F. Goosen, S.S. Sablani, S.S. Al-Maskari, R.H. Al-Belushi, M. Wilf

Effect of feed temperature on permeate flux and mass transfer coefficient in spiral-wound reverse osmosis systems

Desalination, 144 (2002), pp. 367–372

[186] A. Altaee, A. Mabrouk, K. Bourouni
A novel forward osmosis membrane pretreatment of seawater for thermal desalination processes

Desalination, 326 (2013), pp. 19–29

[187] I.H. Huisman, K. Williams
Autopsy and failure analysis of ultrafiltration membranes from a waste-water treatment system

Desalination, 165 (2004), pp. 161–164

[188] A. Sagiv, R. Semiat
Backwash of RO spiral wound membranes

Desalination, 179 (2005), pp. 1–9

[189] V. Puspitasari, A. Granville, P. Le-Clech, V. Chen
Cleaning and ageing effect of sodium hypochlorite on polyvinylidene fluoride (PVDF) membrane

Sep. Purif. Technol., 72 (2010), pp. 301–308

[190] M. Rabuni, N.N. Sulaiman, M. Aroua, C.Y. Chee, N.A. Hashim
Impact of in situ physical and chemical cleaning on PVDF membrane properties and performances

Chem. Eng. Sci., 122 (2015), pp. 426–435

[191] E. Maire, P. Withers
Quantitative X-ray tomography

Int. Mater. Rev., 59 (2014), pp. 1–43

[192] B. Kaouache, F. Addiego, J.-M. Hiver, O. Ferry, V. Toniazzo, D. Ruch
In situ mechanical characterization of short vegetal fibre-reinforced high-density polyethylene using X-ray tomography

Macromol. Mater. Eng., 298 (2013), pp. 1269–1274

[193] J.-C. Remigy, M. Meireles

Assessment of pore geometry and 3-D architecture of filtration membranes by synchrotron radiation computed microtomography

Desalination, 199 (2006), pp. 501–503

[194] F.H. She, D. Gao, W.M. Gao, D.Y. Wu, Z. Peng, M. Hoang, L.X. Kong

Characterization of membranes with X-ray ultramicroscopy

Desalination, 236 (2009), pp. 179–186

[195] H. Reingruber, A. Zankel, C. Mayrhofer, P. Poelt

Quantitative characterization of microfiltration membranes by 3D reconstruction

J. Membr. Sci., 372 (2011), pp. 66–74

[196] J. Viguié, T. Savart, P. Duru, J.C. Rouch, J.C. Remigy

Characterisation of 3D porous macrostructure of hollow fibre membranes using X-ray tomography—effects of some spinning process conditions

J. Membr. Sci., 435 (2013), pp. 11–20

[197] K. Wang, B. Brüster, F. Addiego, G. Kfoury, F. Hassouna, D. Ruch, J.M. Raquez, P. Dubois

Strain-induced deformation mechanisms of polylactide plasticized with acrylated poly (ethylene glycol) obtained by reactive extrusion

Polym. Int., 64 (2015), pp. 1544–1554

[198] F. Addiego, S. Patlazhan, K. Wang, S. André, S. Bernstorff, D. Ruch

Time-resolved small-angle X-ray scattering study of void fraction evolution in high-density polyethylene during stress unloading and strain recovery

Polym. Int., 64 (2015), pp. 1513–1521

[199] K. Schneider, N.E. Zafeiropoulos, M. Stamm

In situ investigation of structural changes during deformation and fracture of polymers by synchrotron SAXS and WAXS

Adv. Eng. Mater., 11 (2009), pp. 502–506
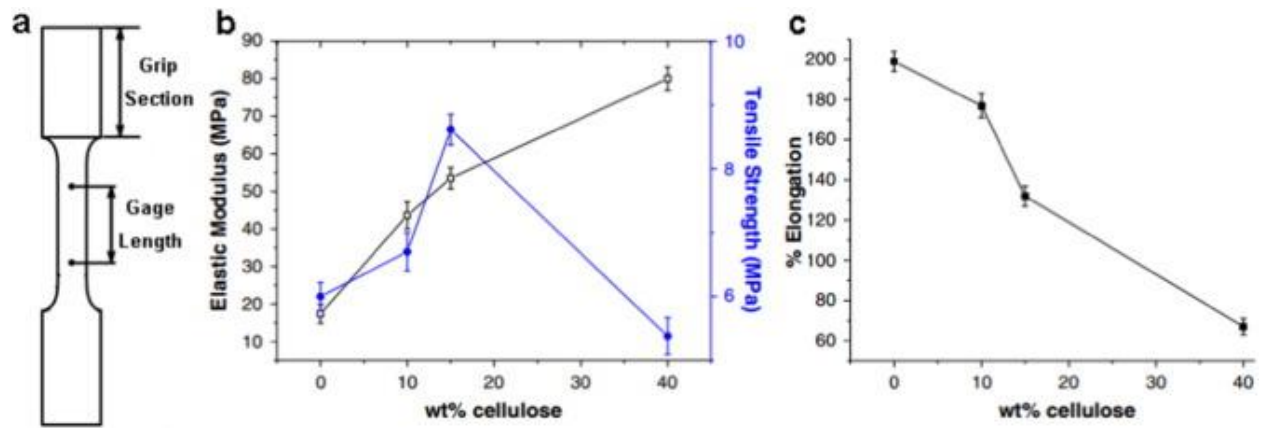
Fig. 1. Effect of cellulose content on the elastic modulus, tensile strength and elongation at break of cellulose/electrospum polyvinylidenefluoride-*co*-hexafluoropropylene (PVDF-HFP) composite membranes. Source [110].
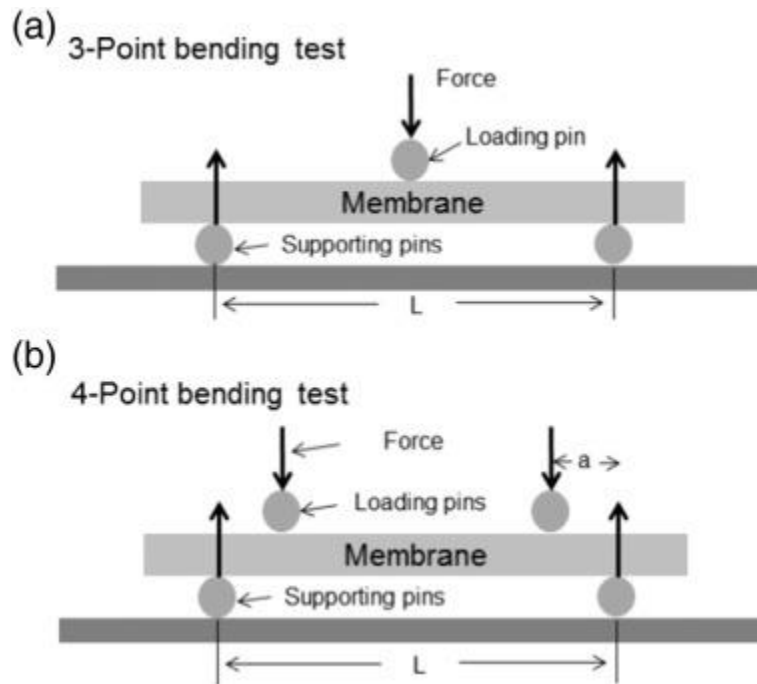

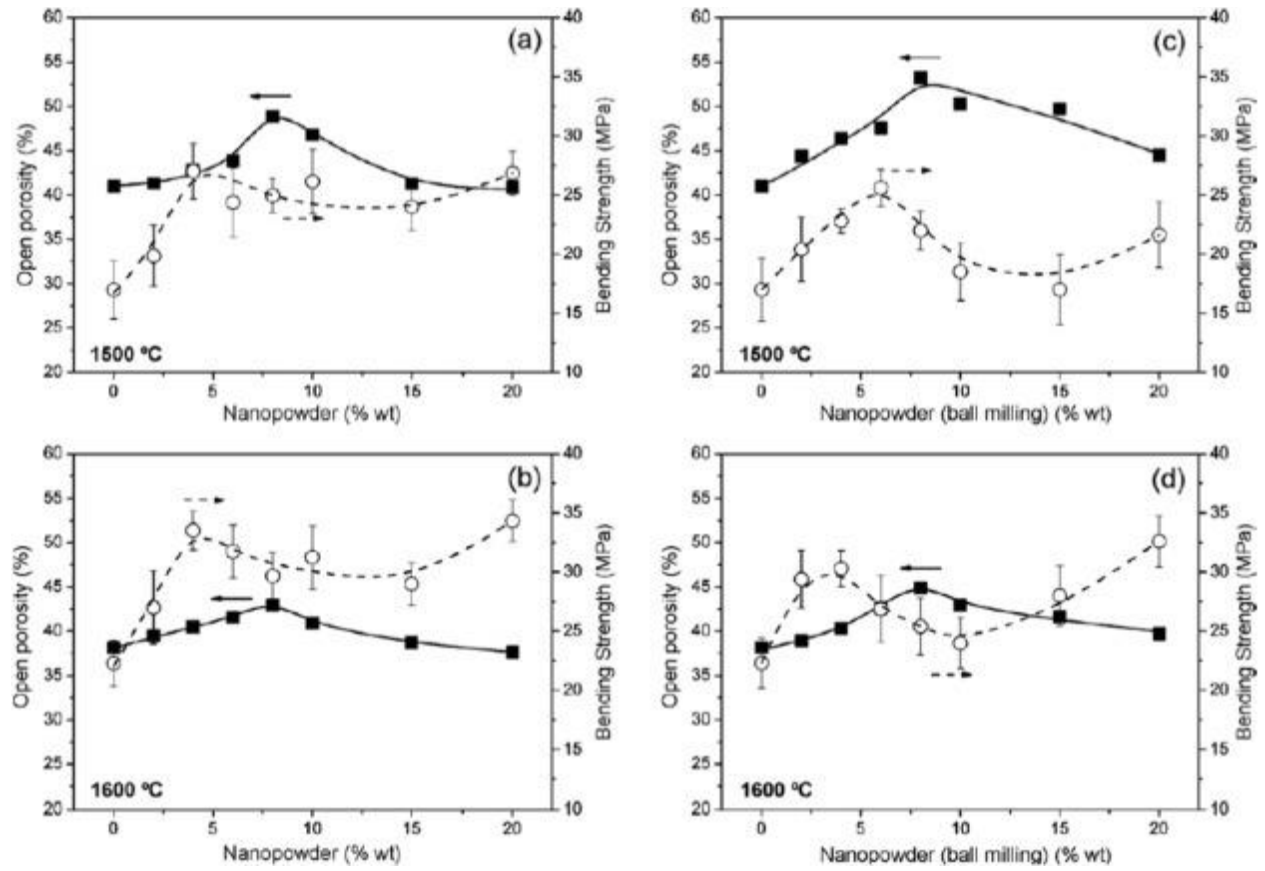Fig. 2. (a) 3-point and (b) 4-point flexure tests for membranes.

Fig. 3. Open porosity and bending strength as a function of the weight percentage of γ-alumina nanopowder in the powder mixture; (a) and (b) ceramics prepared by the simple mixing in the shear mixer sintered at 1500 °C and 1600 °C, respectively; (c) and (d) ceramics prepared by the addition of the ball milling step prior to shear mixing sintered at 1500 °C and 1600 °C, respectively. (■) Porosity; (○) bending strength. Source [66].
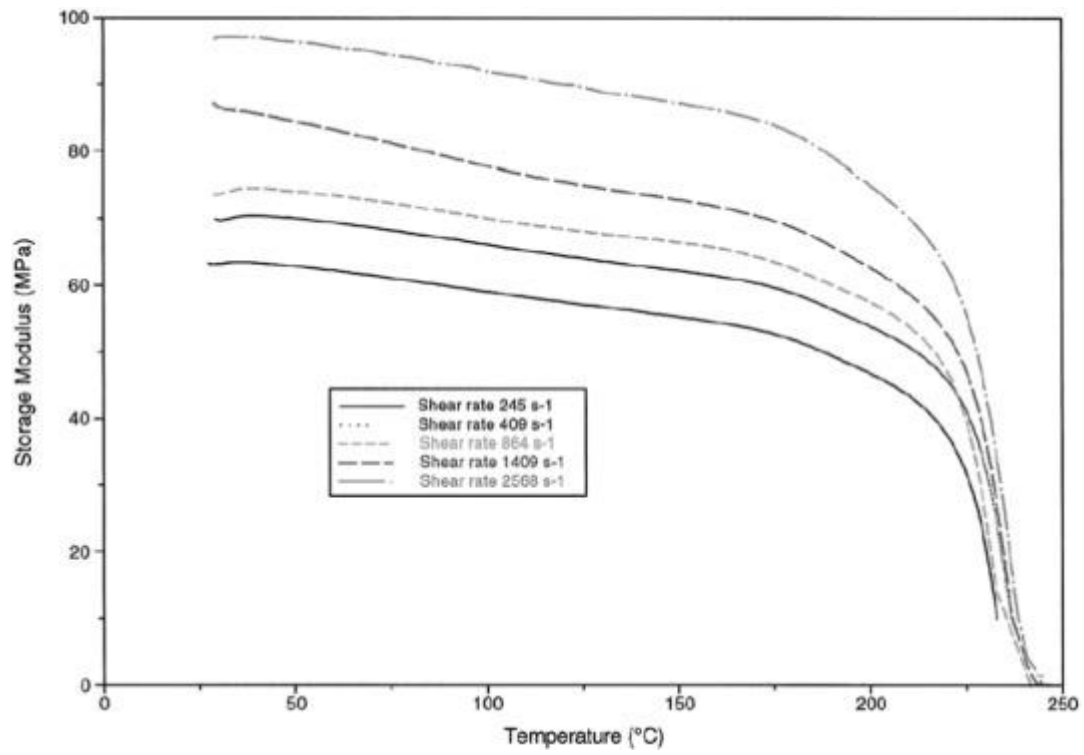
Fig. 4. Storage modulus as a function of temperature for PES hollow fiber membranes with different spinning shear rate. Source [78].
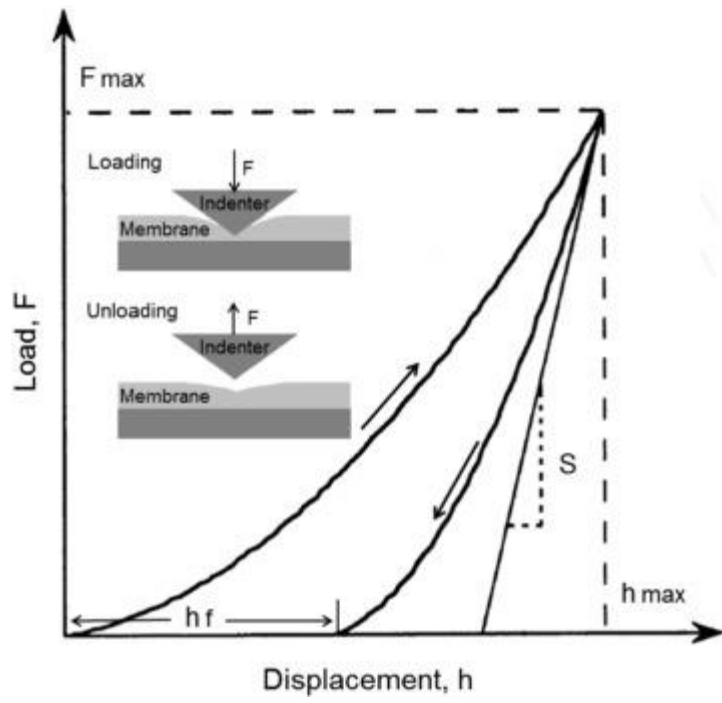
Fig. 5. Typical indentation load–displacement curve.

57
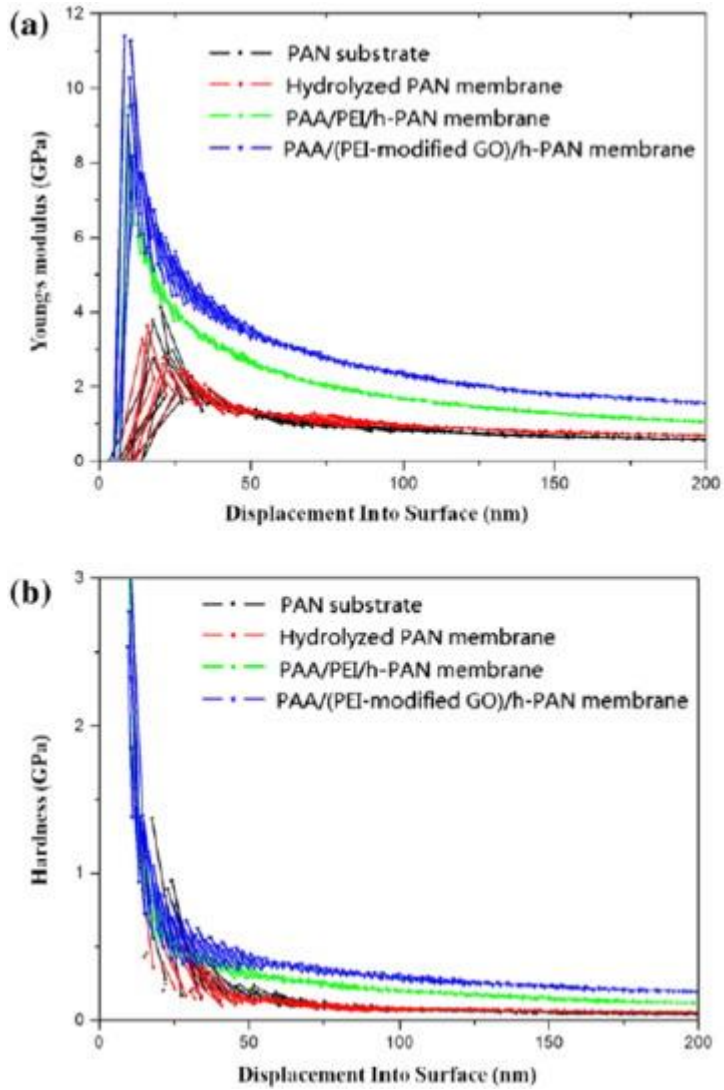
Fig. 6. (a) Young's modulus as a function of displacement into surface with assembly effects. (b) Hardness as a function of displacement into surface. Source [90].
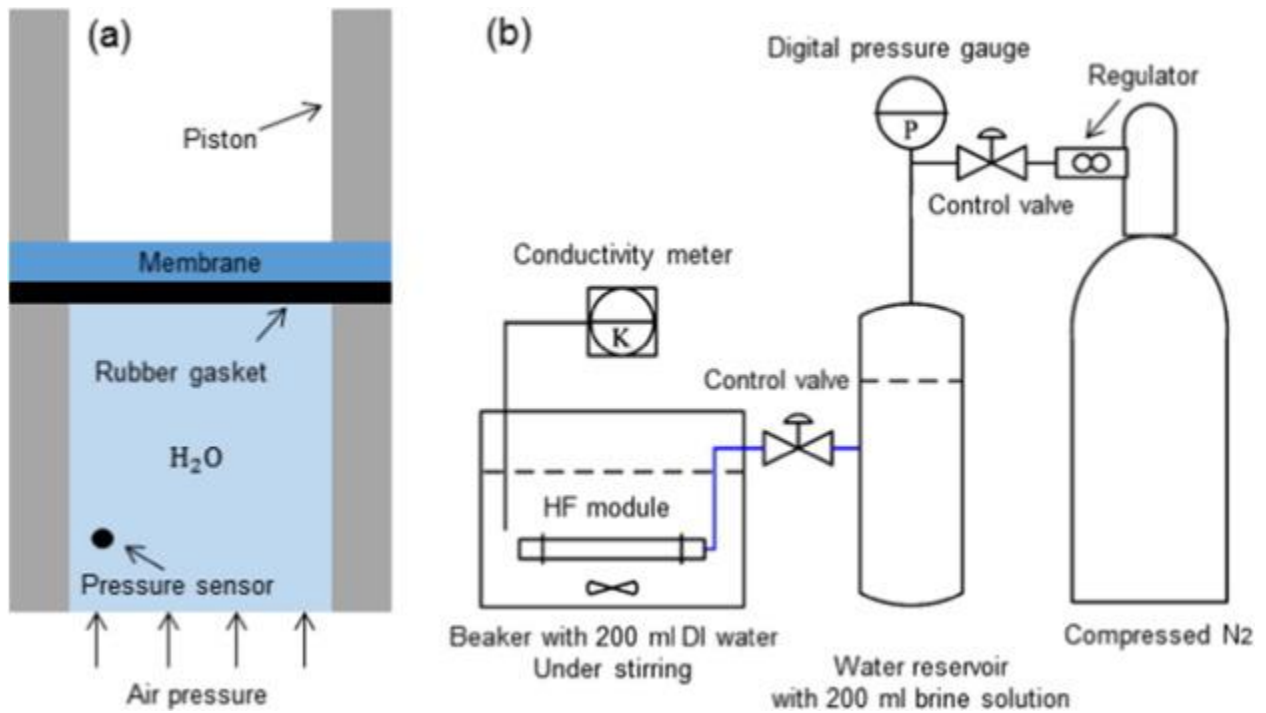
Fig. 7. Illustration of burst pressure measurement setup for (a) flat sheet membrane and (b) hollow fiber membrane. Source [93] and [95].
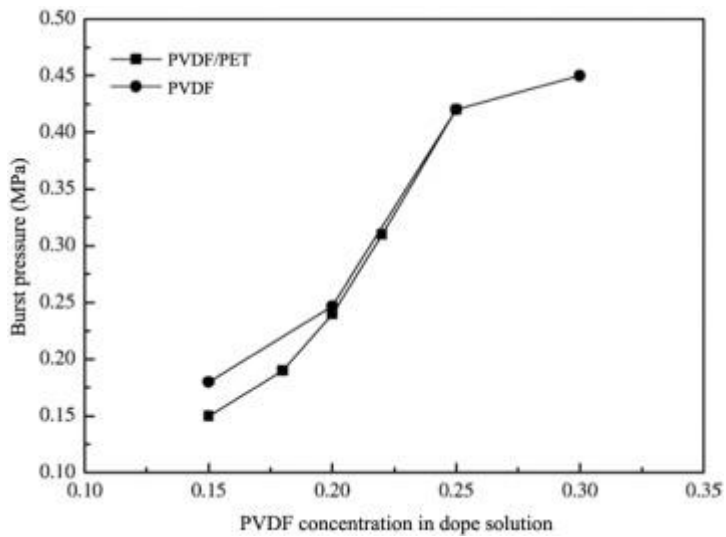

Fig. 8. Effect of PET threads on burst pressure of PVDF hollow fiber membrane with different concentrations. Source [96].
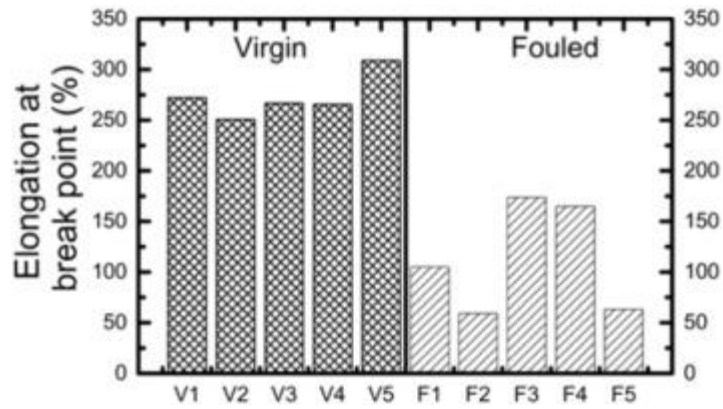
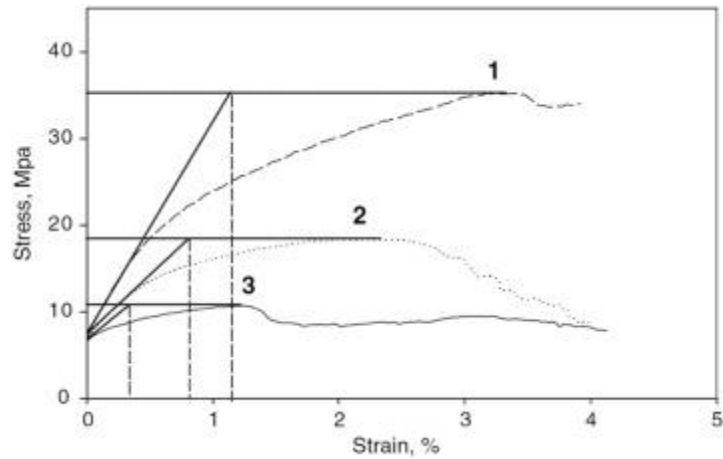Fig. 9. Elongation at break of five fouled hollow fiber membranes compared to virgin ones. Source [151].

Fig. 10. Uniaxial tensile curves for the pristine CA membrane (1) and CA membranes cleaned with hypochlorite 5 g h/L (2) and 18 g h/L (3). Source [157].
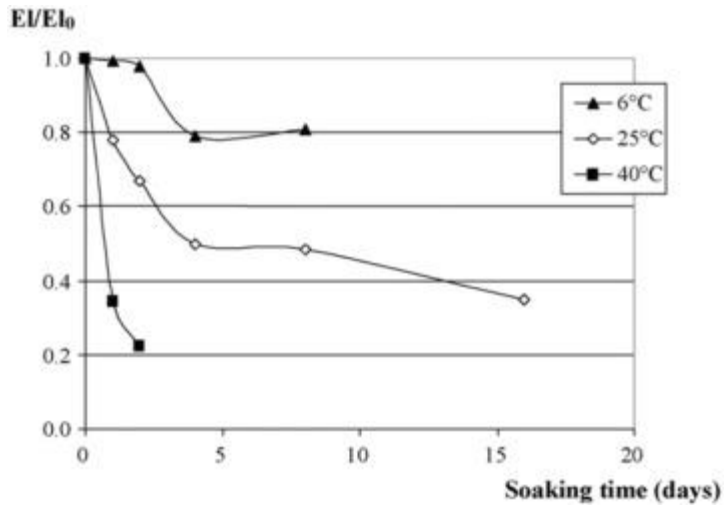
Fig. 11. Relative elongation at break of PSF membranes immersed in hypochlorite solutions at 100 ppm HClO, pH 7, and various temperature, $El_0 = 37\%$. Source [160].
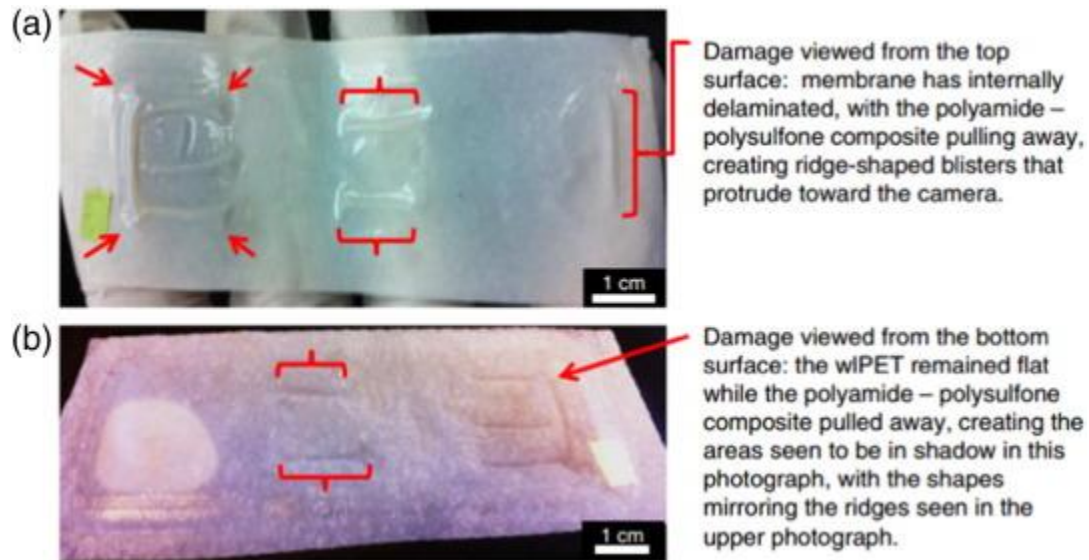

Fig. 12. Digital photographs of wet-laid thin film composite membrane after test for response to shear stress induced by moderate cross-flow velocity. Delamination at the PET–PSF interface is seen from (A) the top surface and (B) the bottom surface. The delamination shown occurred in a cell with counter-current flow of deionized water at cross-flow velocities that were gradually increased up to 26 cm/s. Source [166]

61

List of Tables:

Table 1. Summary of the applications, materials, configurations of water treatment membranes and typical test methods for assessment of their mechanical properties.

Application	Membrane materials	Membrane configurations	Typical mechanical test methods	Membrane mechanical investigation used for
Drinking water treatment	Metal	Tubular	Uniaxial tensile test	Membrane design
Wastewater treatment	Ceramic	Plate and frame	Bending test	Diagnosing performance
Desalination	Polymer	Hollow fiber	Dynamic mechanical analysis	Durability/degradation evaluation
		Spiral wound	Nanoindentation	Membrane integrity
			Bursting test	Fouling/scaling evaluation

Table 2. Tests used for mechanical characterization of water treatment membranes and the reported mechanical properties.

Approaches	Based materials	References	Reported Mechanical properties
Uniaxial tensile test	PVDF	[32–45]	Stress–strain curve, Young's modulus, yield stress, ultimate stress, elongation at break, fracture toughness
	PAN	[46,47]	
	CA	[48]	
	PES	[49–53]	
	PSF	[54–59]	
	PAI	[22]	
	PVA	[60]	
	PP	[61–63]	
	Chitosan	[64,65]	
Bending test	Al2O3	[66–70]	Bending strength, fracture toughness
	Kaolin	[71–75]	
	Nickel	[76]	
	ZrO2	[77]	
Dynamic mechanical analysis	PES	[50,53,78–80]	Storage modulus, loss modulus
	PVA	[81,82]	

Approaches	Based materials	References	Reported Mechanical properties
	PVDF	[83]	
	PET	[84]	
	SPES	[85]	
	PU	[86]	
Nanoindentation	Clay	[87]	Young's modulus, hardness
	PES	[80,88]	
	PS	[89]	
	PAN	[90]	
	Carbon	[91]	
	AQPz	[92]	
Bursting test	PVDF	[93–96]	Bursting strength
	PES	[97]	
	CMS	[98]	
	PLA	[99]	
	PSF	[100]	
	PEI	[101]	